Independent Evaluation of the Critical Initial Flaw Size for Ares I-X (AIX) Upper Stage Simulator (USS) Common Segment Flange-to-Skin Welds

February 26, 2008

Approval and Document Revision History

Approved:	Original signature on file	3/20/08
	NESC Director	Date

Version	Description of Revision	Author	Effective Date
Base	Initial Release	Derrick Cheston, NESC Chief Engineer	February 26, 2008

Table of Contents

Volume I: Consultation Report

Volume II: Appendices

List of Figures

List of Tables

Volume I: Assessment Report

1.0 Authorization and Notification

The Ares I launch vehicle will be flight tested to gather performance data associated with Ares I First Stage. Ares I-1 will include a live, four-segment Solid Rocket Motor booster, a functional roll control system, and a separation ring. The NASA Engineering and Safety Center (NESC) in conjunction with the Ares I-1 Upper Stage Project developed a representative load spectrum for the Ares I-1 Upper Stage Simulator/Spacecraft Adapter/Service Module (Ares I-1 USS). The Ares I-1 USS is an all welded structure. As such critical initial flaw size for imperfections, flaws, or cracks in the welds needed to be determined to ensure that the USS structure will not experience catastrophic failure. The NESC provided independent evaluation, expert advice, and guidance to the Ares I-1 Upper Stage Project in key areas such as welding residual stress, fit-up stress, and material property evaluation. The NESC also used the above information to determine the critical initial flaw size (CIFS) for the Ares I-1 USS structure. This assessment was approved out of board on March 14, 2006 by Ralph Roe, NESC Director, and assigned to Derrick Cheston, NESC Chief Engineer, as the Lead.

The NESC Team was tasked to perform an independent review of data and provide consultation on the following:

1) To provide an independent evaluation of the approach to fracture control for the Ares I-1 USS.[1]

2) Perform an independent analysis and necessary material testing as well as evaluation of the approach taken to compute the CIFS.

[1] The NESC independent evaluation of the AIX USS fracture control approach was a by-product of this assessment report. In addition, general consultation on fracture control was provided throughout the NESC team's engagement with the AIX USS Project through Technical Interchange Meetings (TIM) and NESC participation in the AIX Charge 1design review.

2.0 Signature Page

Mr. Derrick Cheston	Date	Dr. Ivatury Raju	Date
Dr. Robert Piascik	Date	Mr. Sam Russell	Date
Dr. Curtis Larsen	Date	Dr. Stephen Hudak	Date
Dr. Norman Knight	Date	Mr. Walter Reuter	Date
Dr. Frederick Brust	Date	Dr. David Dawicke	Date
Mr. James Womack	Date	Mr. Michael Hayes	Date
Ms. Dawn Phillips	Date		

3.0 List of Team Members

Name	Position/TDT Affiliation	Center/Contractor
Core Team		
Derrick Cheston	Team Lead, NESC Chief Engineer	NASA, GRC
Ivatury Raju	Structures Technical Fellow	NASA, LaRC
Robert Piascik	Materials Technical Fellow	NASA, LaRC
Curtis Larsen	Loads & Dynamics Technical Fellow	NASA, JSC
Alden Mackey	Loads and Dynamics	Barrios Technology
Stephen Hudak	Materials TDT	Southwest Research Institute
Walt Reuter	Materials TDT	ATK
Sam Russell	NDE TDT	NASA, MSFC
Frederick Brust	Structures TDT	Battelle/Engineering Mechanics Corporation of Columbus
Dave Dawicke	Structures TDT	AS&M, LaRC
Norman Knight	Structures TDT	GD-AIS, LaRC
Pappu Murthy	Structures TDT	NASA, GRC
Dawn Phillips	Structures TDT	Lockheed, LaRC
James Womack	Statistics TDT	The Aerospace Corporation
Michael Hayes	Welding Consultant	Acute Technologies Services, LCC
Jane Manderscheid	Project Liaison	NASA, GRC
Support Personnel		
Chris Johansen	Program Analyst	NASA, LaRC
Christina Cooper	Technical Writer	ATK, LaRC
Lisa Behun	Planning and Control Analyst	ATK, LaRC

4.0 Executive Summary

The NASA Engineering and Safety Center (NESC) was requested to independently evaluate the critical initial flaw size (CIFS) in the welds in the common segments of the Ares I-X Upper Stage Simulator (AIX USS). The purpose of the request was to obtain data to guide the post-weld-inspection procedures and methods. The AIX Project desired to use standard[2] non-destructive evaluation techniques to evaluate the welds, an approach that is valid only if the CIFS is larger than the detectable size of standard inspection methods. In addition, the AIX Project planned to use the calculated CIFS to develop pass/fail criteria by which the welds would be considered acceptable, unacceptable or require a repair.

The NESC collaborated with the AIX Project and the Ares Vehicle Integration Office (AVIO) to establish a set of loads spectra (cycles of axial forces and moments) to bound the expected loads in the rollout, pad stay, liftoff, and ascent environments. In addition, the NESC in conjunction with the AIX USS Project developed a set of load spectra for the transportation and handling environments. The location of maximum equivalent tensile line loads was determined to occur among the common segments at the US-1/US-2 interface. The equivalent loads were applied to finite element structural models to determine the maximum crack-opening stress locations.

The NESC assumed the most likely weld defect of concern would be slag inclusions, or a surface or an embedded crack caused by a lack-of-fusion on the sidewall. The NESC team modeled these defect geometries assuming linear-elastic materials response and using the linear-elastic fracture mechanics (LEFM) concepts in the NASGRO code [3] to compute the crack growth rate and number of load cycles to failure in the welded structure.

Parametric NASGRO analyses were performed for several initial crack sizes and geometries, local stress conditions and material properties to determine the sensitivity of the CIFS predictions to these key input variables. The NESC determined that the CIFS is strongly dependent upon the materials' fracture toughness as well as the assumed magnitude of fit-up and residual stresses. Therefore, the NESC conducted independent fracture toughness testing of the welded samples provided by the AIX USS Project. The NESC also performed independent analytical predictions of the weld residual stress and fit-up stresses based upon the welding and assembly procedures, respectively, that were defined by the AIX USS Project.

[2] Pursuant NASA-STD-(I)-5009 Nondestructive Evaluation Requirements for Fracture Critical Metallic Components, standard non-destructive techniques have established statistically based flaw detection capabilities (e.g., fluorescent penetrant, radiography, ultrasonic, eddy current, and magnetic particle.)

The CIFS value was calculated to be highly sensitive to the value of the weld fracture toughness. The larger the value of fracture toughness, the larger is the CIFS. In order to maintain consistently high fracture toughness values in the weld, quality control of the manufacturing process was shown to be imperative. For example, the NESC recommended that the AIX Project procure weld wire from a single lot and maintain stringent storage with environmental control for the flange-to-skin welds. It was also recommended that the AIX Project perform sufficient (pre-declared confidence) testing to determine the fracture toughness values for the specific final welding procedures for all fracture-critical welds.

NESC recommends the use of a surface crack CIFS of 0.084 inch in the depth direction for the development of weld inspection criteria for the flange-to-skin weld. The NESC also recommends that the AIX Project perform volumetric inspection that is capable of detecting both surface and embedded cracks of this CIFS magnitude from sidewall lack-of-fusion and slag inclusion.

However, it is important to point out that the fracture toughness values for the flight-like weld design have not been characterized; thus, the NESC's CIFS analysis employed what was believed to be a conservatively low assumed value for fracture toughness based on data from a different welding procedure. Consequently, it is essential that the AIX Project measure the fracture toughness on coupons representative of the final welding process to be used in fabricating the AIX USS.

The NESC further recommends that the AIX Project assess the weld integrity at other interfaces in the USS to determine the level of criticality, and utilize a similar approach to that demonstrated in this report to determine the CIFS for other critical weld joint designs. In addition, the NESC recommends that repair welds be designed and that the final passes are deposited so as to develop a favorable residual stress distribution [e.g. on the outer diameter (OD) of the weld joint].

5.0 Assessment Plan

The NESC formed a team consisting of members provided by the following NASA Technical Fellows and their respective Technical Discipline Teams (TDTs): Loads, Structures, Materials, and Non-Destructive Evaluation (NDE), as well as statistical experts. The team was augmented by a welding consultant from the off-shore oil industry having extensive experience in the welding of structural steels. The approach taken to evaluate the CIFS was to use industry- and NASA-accepted methods for conducting fatigue and fracture analyses, which are outlined in later sections of this report.

This NESC assessment was conducted concurrent with the design, analysis, and initial manufacturing of flight hardware by the AIX Project Team. As a result, the as-built hardware in some cases varies from the as-analyzed design consequently results may not be entirely applicable to the final as-built hardware. Thus, an important goal of this report was also to thoroughly documents the approach employed and assumptions utilized, as well as highlights the primary variables that can influence the CIFS. In this way the report will provide a resource for the AIX USS Project team to identify and assess the impact of any changes in design and/or fabrication that may have evolved during the course of this NESC assessment, as well as following this assessment.

6.0 Description of the Problem and Proposed Solutions

6.1 Description of the Problem

The AIX USS represents the Upper Stage of the Ares I vehicle in mass, center-of-gravity, and outer mold line. To achieve a low manufacturing cost, the USS is designed in a modular fashion consisting of cylindrical segments made of 1/2 inch thick construction grade A516 Grade 70 plate steel. Machined flanges are welded onto either end of the cylindrical segments for bolting adjacent segments. The flange-to-skin (or flange-to-shell) weld is one of several weld joints used in the design of USS. The flange-to-skin weld is located at the outermost diameter and is in the primary load path of the flight test vehicle. At the time of the request to the NESC, the AIX USS Project's design and manufacturing procedures were in the early stages of development. A prototype referred to as Pathfinder One had been fabricated and the welds had undergone inspection. As a result of inadequate weld quality experienced on Pathfinder One, the AIX USS Project began taking measures to improve weld processes and to establish the weld acceptance criteria. This led to the need to identify the weld CIFS.

From a simplified standpoint, NASA-STD-5019 (Reference 1) requires that critical structures be designed so that the largest crack (CIFS) that can be missed, (within a given confidence bound) by the NDE technique, not grow to the critical length within 4 design life times. Figure 6.1-1 shows a hypothetical crack length versus cycle curve. The critical flaw size (CFS) is the crack length that results in a stress intensity factor that exceeds the material's fracture toughness. Fracture mechanics is used to analytically estimate the CIFS by integrating information on applied stresses, hypothesized crack sizes and shapes, as well as material properties including fatigue crack growth rates and fracture toughness.

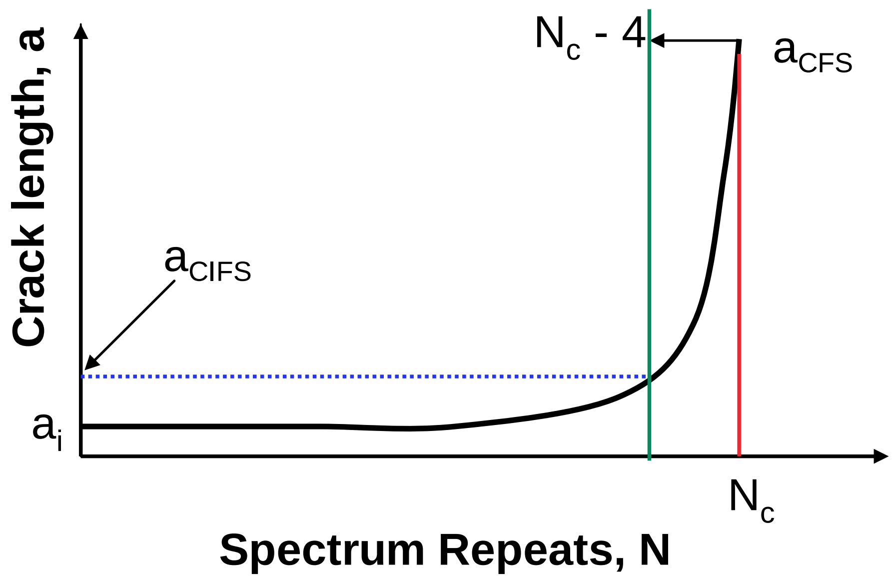

Figure 6.1-1. Illustration of Critical Flaw Size (CFS) and Critical Initial Flaw Size (CIFS) for a Hypothetical Crack Length versus Cycles Curve

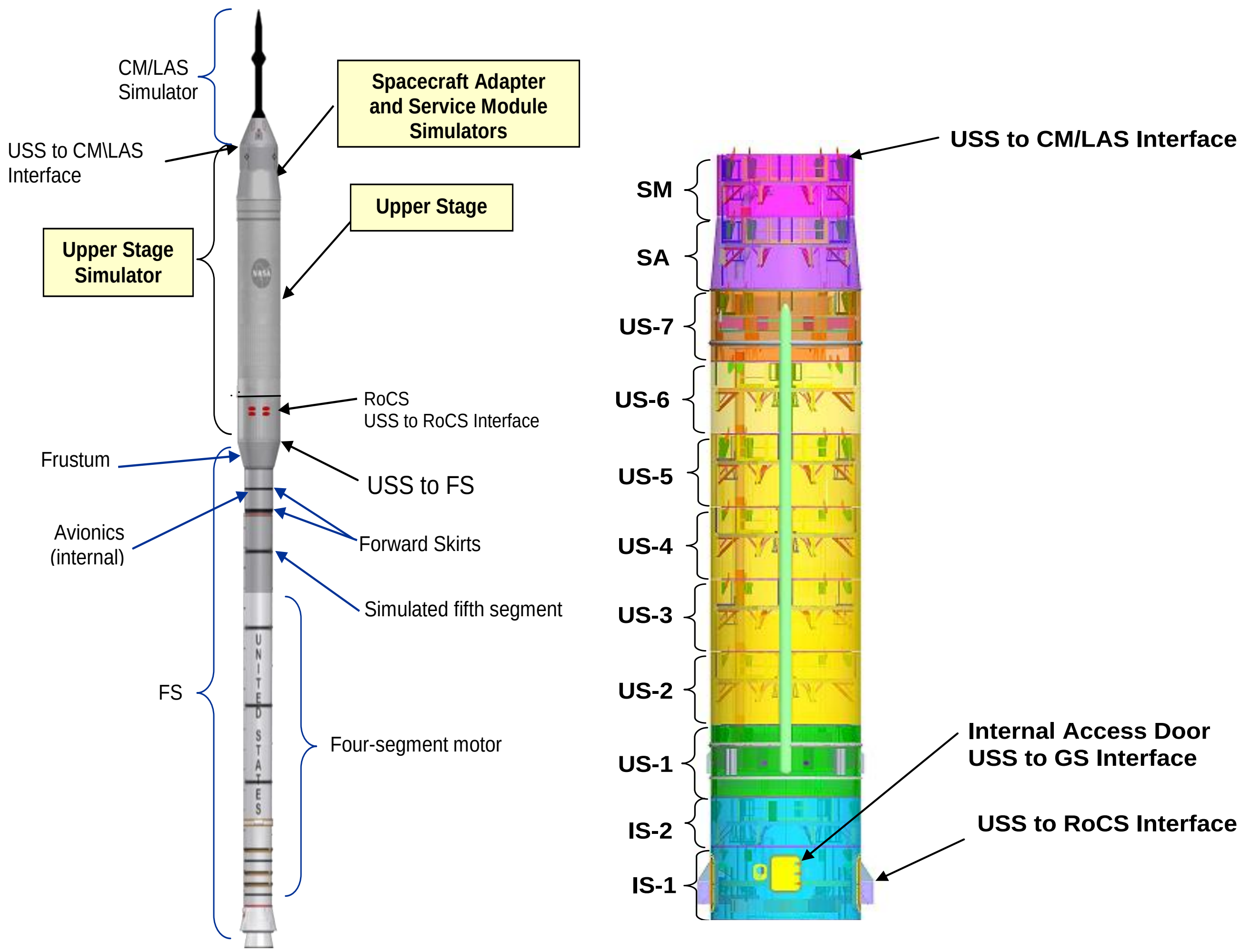

Figure 6.1-2. Ares I-X Vehicle Stack with Upper Stage Simulator Highlighted and USS Segments

6.2 Scope

The AIX USS Project is responsible for development of all of the AIX vehicle structure between the First Stage (FS) forward frustrum and the simulated Crew Module (CM). At the time of this request, and for purposes of this report, the CIFS evaluated by the NESC team only applied to the welds within the common segments designated US-1 through US-7 whose shell and flange designs were identical. The NESC team specifically focused on the US1/US2 interface welds. Also, this analysis did not evaluate the welded structure of the interstage sections (IS-1, IS-2) nor the simulated spacecraft adapter, or simulated service module. These components were designed and manufactured in a similar manner, but are have significantly different geometry and loads.

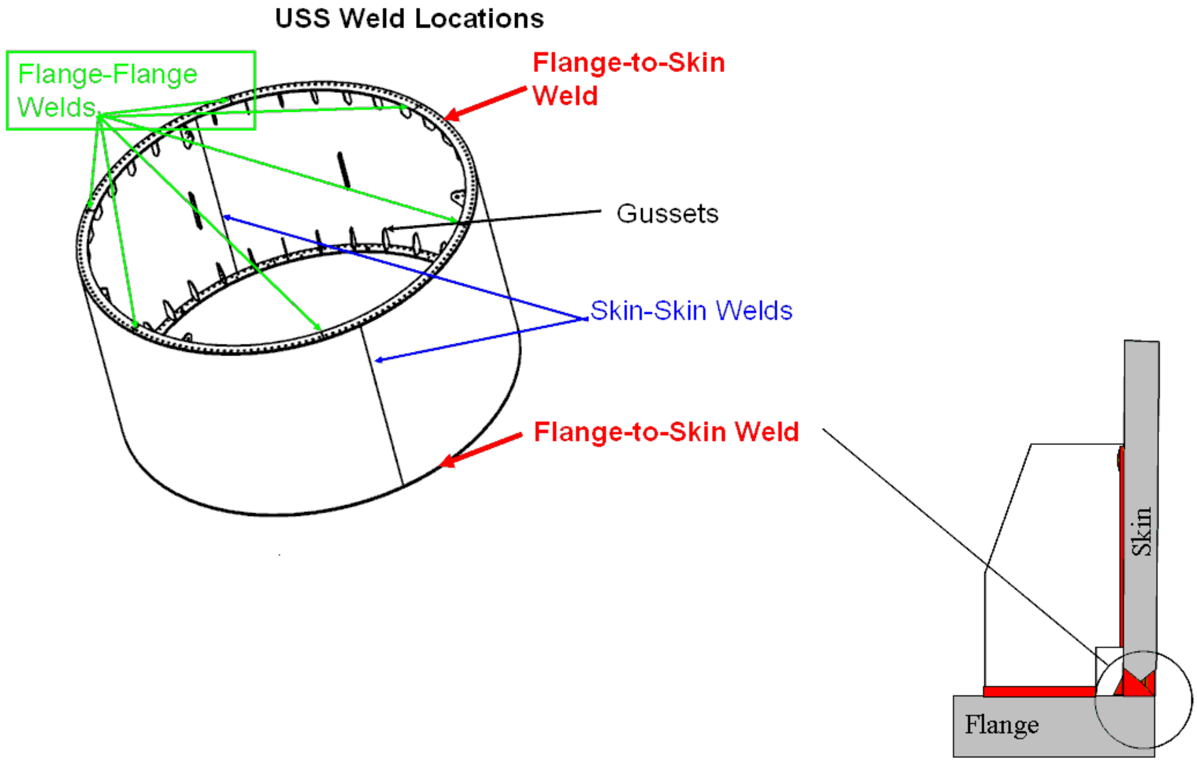

Figure 6.2-1. Ares I-X Vehicle Upper Stage Simulator Common Segment Typical Weld Locations

6.3 Proposed Solutions

The AIX USS Project developed a fracture risk mitigation plan that focuses on a strategy of mitigating fatigue crack growth and fracture initiated from welding defects in the USS welded joints. The mitigation strategy was addressed in terms of the design approach and manufacturing approach. The AIX USS Project design approach focused on the use of established weld standards and codes, the selection of parent material, and supporting fracture analyses. Both deterministic damage tolerance analysis to predict the CIFS and a probabilistic analysis to determine the sensitivity of the CIFS to process variability were considered.

The risk mitigation plan identified the use of damage tolerance analytical methods including NASGRO to determine the initial level of damage/defect in the weld that would be tolerated by the structure over the required life time. The AIX USS Project proposed to adopt the American Weld Society (AWS) D1.1 standard for weld acceptance criteria. However, the acceptable flaw required by AWS D1.1, while assumed to be conservatively small, was expected to be difficult to achieve based upon the experience level of the welders and could result in a higher than desired number of weld repairs.

The AIX USS Project approached the solution according to its risk mitigation plan. The material selection and the conservative factors of safety chosen are part of the design risk mitigation plan. The AIX USS Project initiated the deterministic CIFS analysis. The AIX USS Project, recognizing the importance of the welded joint structural integrity analysis, also requested an independent CIFS assessment by the NESC.

6.4 Risk Assessment

The NESC did not perform a separate risk assessment independent of the AIX USS Project. The AIX USS had identified structural failure as its top risk at the time of the request with an assigned Likelihood rating of three and a Consequence rating of five on a five by five risk matrix. The risk statement is shown below.

- **Risk US-5: Ares I-X USS Fracture -** Given that a flaw larger than the CIFS could originate in any load bearing structural component, there is a possibility that the flaw could propagate, potentially resulting in loss of the vehicle.

7.0 Data Analysis

7.1 Solution Methodology Approach

The NESC team began with the assumption that the smallest CIFS would be in the Common Segment flange-to-skin weld. This assumption was based on an examination of stress analyses performed by the AIX USS Project. Following this assumption, the NESC's CIFS assessment focused on the critical flange-to-skin weld joint in the Common Segment.

- **O-1 Only the analysis of the flange-to-skin joint of the Common Segments was performed by the NESC team. Other segments may have welds fabricated by other means than the weld that was evaluated and/or with higher local stress values (e.g. Interstage Segments).**

The NESC team approached the AIX USS Project request by following the general procedure outlined in Figure 7.1-1. Load cases were identified and estimated for handling, assembly, ground transportation, rollout, pad stay, liftoff, and ascent flight conditions. From the loads analysis, the NESC team determined the location within the common segments that the maximum combined resultant tensile load occurs, as described in Appendix D. This maximum resultant load was applied to a detailed finite element model of the simulated weld joint and the maximum stress condition in the weld was determined, as described in Appendix B. Similar finite element models were used to predict the residual stresses from assembly and welding processes see Appendices B and E. A weld defect with a crack depth equal to a_i and surface length equal $2c_i$ was assumed to be located at the maximum stress location and was oriented normal to the maximum stress direction as calculated by the finite element analysis. The cyclic spectrum loads (discussed in section 7.2) were applied to this crack configuration repeatedly and NASGRO was used to perform the crack growth calculations. The crack size, shape, and the maximum value of stress-intensity factor (K) were monitored until the K-value reached the material fracture toughness. From a plot of crack length versus equivalent life cycles, the location of the CIFS was determined by marching backward along the curve from the CFS to the location on the curve that was four complete life cycles prior the point of critical stress-intensity as shown in Figure 7.1-1. This location represents the CIFS on the largest crack that would survive four complete repeats of the lifecycle spectrum.

General Procedure for Determination of CIFS

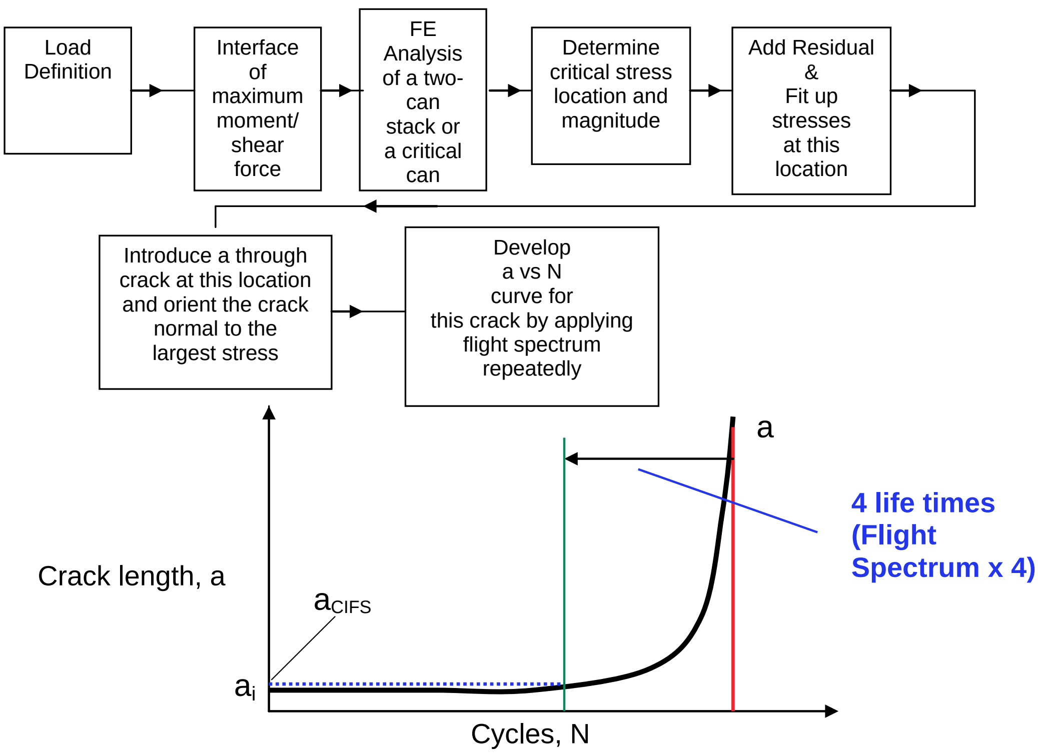

Figure 7.1-1. General Procedure for Determination of CIFS

The following major assumptions were made in computing the critical initial flaw size for this application.

- Application of linear elastic fracture mechanics (LEFM) is valid for this analysis case
- Peak tensile and compressive axial loads occur at the same circumferential location
- Axial stresses, residual stresses, and fit-up stresses are constant along the circumferential direction
- Weld and fit-up residual stresses remain constant during crack growth
- The fracture toughness is equal to the elastic component of the J_{IC} determined from tests on a single-bevel weld
- Fatigue crack threshold effects ignored
- Load interaction effects ignored
- Interaction effects such as crack growth retardation are ignored

- Weld peaking and mismatch was ignored
- Defect proximity was ignored
- Worst case-fit-up stresses were assumed
- The net-section stress equal to flow stress criteria in NASGRO was bypassed

7.2 Loads Analysis

At the onset of the NESC assessment, a mutual agreement was established with the AIX USS Project that although the NESC team would independently model the structure and develop stress distributions and determine resulting CIFS, a consistent set of loads and application frequencies would be used by both teams to determine the loads spectra to be used for the life analysis. At the time, a complete set of prelaunch, liftoff, and ascent loads for the AIX vehicle did not exist. Therefore, the NESC team worked in partnership with the AVIO Loads and Dynamics engineers, the Constellation Program's Ares I Loads Panel, and the AIX USS Project structures team to develop a set of bounding loads spectra for fracture mechanics modeling and CIFS prediction.

The most comprehensive set of design loads existing at the time were identified as the "mini-loads cycle" results for the Ares I vehicle documented in the MSFC Engineering memo EV30-07-001 "Preliminary Design Loads for Ares-I Design Analysis Cycle 2 (ADAC-2)". The loads provided by this memo resulted from response analyses of pre-launch (pad stay winds), liftoff, and ascent flight design environments. Because the design of the Ares I and AIX vehicles did not precisely match, the NESC used the available finite element models of the AIX and Ares I vehicles to interpolate the loads for the AIX USS joint locations. To develop load spectra estimates from these design cases, the design load in each flight regime was proportioned according to rationale appropriate to the flight phase and a number of cycles were assigned. For example, for liftoff, a ten-second response of the 1 Hz primary free-free bending mode was assumed, with the peaks decaying according to an assumed 1 percent damping ratio. Similarly, for ascent, a 70-second period of significant dynamic pressure [q > ~350 pounds per square foot (psf)] was determined from a typical Ares-I predicted ascent trajectory and the maximum design bending moment was assumed to occur at maximum q. Ten equally spaced wind events were assumed to occur in this period with the induced vehicle bending moment determined as the design bending moment proportioned by the ratio of q at that time to the maximum q. A peak decay based on one percent damping was used in each of the ten 7-second time periods.

For the rollout spectra, a special response analysis of an Ares I vehicle transported by a crawler-transporter on a Space Shuttle Mobile Launch Platform was commissioned from the Johnson Space Center (JSC) Engineering Loads and Structural Dynamics Branch. The resulting load cycles were identified and counted using a rainflow algorithm. The assumptions and the basis for each load spectrum regime are summarized in Table 7.2-1. Further details are provided in Appendix D.

Table 7.2-1. Loading Events

Load Spectrum	Source of Predicted Loads	Scenario Described
Lifting	A conservative envelope of the concept of operations for handling and assembly.	Single 1.5X proof load, 11 multiple segment lifts, and 42 single segment lifts.
Transportation	Shipboard transportation data.	50 day transport from Glenn research Center (GRC) to the Kennedy Space Center (KSC).
Roll-Out	Forced response of an Ares I with fueled US model using forcing function inputs defined from a Space Shuttle Solid Rocket Booster (SRB) stack roll-out test.	Assumed five round trips between the Vehicle Assembly Building (VAB) and pad followed by one final trip to pad.
Pad-Stay	Ares I Preliminary Ares Design and Analysis Cycle (ADAC)-2 Loads.	Total 300 day pad stay plus a single design gust load.
Liftoff	Ares I Preliminary ADAC-2 Loads.	10 second duration of the first mode response.
Ascent	Ares I Preliminary ADAC-2 Loads.	10 events in 70 second duration of significant dynamic pressure.
Thrust Oscillation	Space shuttle critical mass model.	Based upon ground and flight data for reusable solid rocket motor (RSRM).

Equivalent line loads around the shell were calculated at various stations X on the USS based upon the simultaneous combination of minimum (or tensile) axial forces and maximum moments. This resulted in the generation of overall peak tensile and compressive axial forces and moments. The location consistent loads were combined at a given cross section, but the time consistent loads were not used in order to provide an upper bound load state (i.e., the cyclic load range was determined from the peak tensile and peak compressive loads). The distribution of the equivalent maximum line load (Nx) for the rollout, pad stay, liftoff, and ascent events is shown in Figure 7.2-1 as a function of the USS longitudinal (X-axis) coordinate. Negative values indicate net equivalent tension loads. The US-1/US-2 interface corresponds with location X =1693 that was determined to have the overall maximum tensile line load of 1600 pounds per inch (lb/in.) due to the liftoff event.

- **F-1 Peak tension load occurs during liftoff at the US1/US2 interface with a predicted magnitude of 1600 lb/in.**

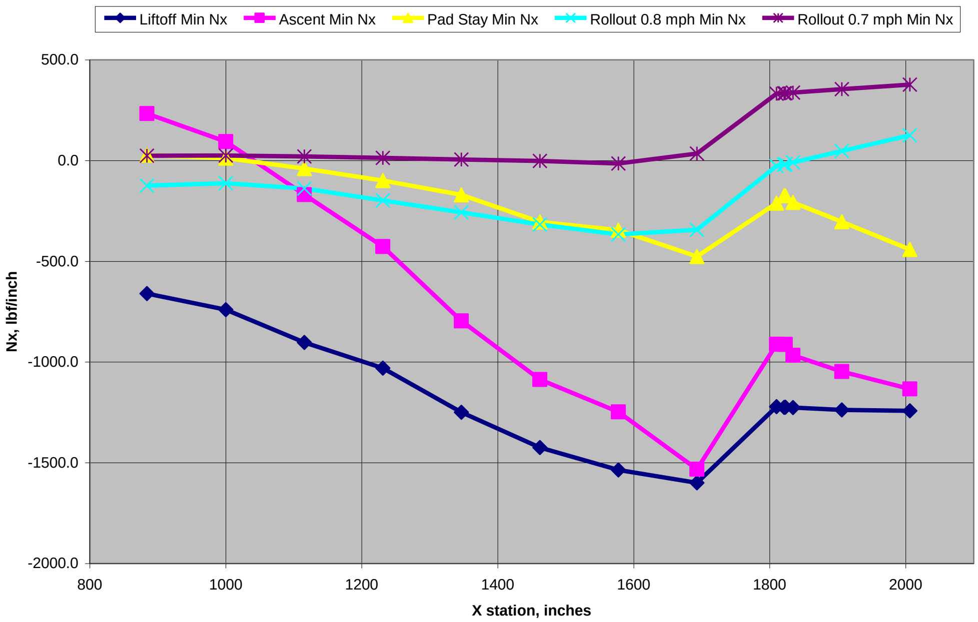

Figure 7.2-1. Equivalent Line Load (Nx) Distribution

In addition to the liftoff event, the US-1/US-2 interface had peak or near peak line loads for ascent, pad stay, and rollout events. Thus, the equivalent loads at the US-1/US-2 interface were used for all load regimes as the controlling loads for computing cyclic stresses for CIFS analysis purposes. The loads that occur at the US-1/US-2 interface are summarized in Table 7.2-2.

Table 7.2-2. Loads at the US-1/US-2 (Units in Table)Interface*

	Max N_x (lb/in)	Min N_x (lb/in)
Lifting: Proof Load	-1092	1092
Lifting: Multi-segment	-728	728
Lifting: Single segment	-243	243
Transportation	-76	76
Rollout (0.8 mph)	-370	740
Padstay - Peak Wind	-809	1554
Padstay 100%	-476	914
Liftoff	-1600	2275
Thrust Oscillation	-120	120
Ascent	-1532	2785

*Note: *Negative values denote tensile loading.*

7.3 Linear Elastic Stress Analysis

The loads analysis indicated that the joint between the US-1 and US-2 segments (X = 1693, see Figure 7.2-1) was the most heavily tensile loaded common USS segment. The analysis focused on this joint interface and a finite element stress analysis using ABAQUS[3] was initiated to determine the peak local stress location and magnitude. The details of this analysis are presented in Appendix B.

Welding and assembly 'fit-up' (primarily mismatch of non-planer flange surfaces) can generate residual stresses. A comprehensive modeling of the weld process was conducted to determine the weld residual stresses, as described in Appendix E. The fit-up stresses were determined by detailed finite element analyses of the flange mismatch, as described in Appendix B. These residual stresses were not functions of the load spectrum and hence were treated as a mean stress in the crack growth (NASGRO) analysis.

LEFM assumptions were used in the NASGRO analysis. An elastic plastic fracture mechanics (EPFM) analysis confirmed that the LEFM assumptions resulted conservative CFS, and thus CIFS predictions for the most critical crack geometry (see section 7.6). Details of the EPFM analysis are presented in Appendix F.

[3] ABAQUAS is a general purpose finite element program.

7.3.1 Cyclic Stress

The peak tensile stress in the flange-to-skin weld for the liftoff event (maximum tensile line load of 1600 lbs/in.) was approximately 13 ksi. The corresponding peak compressive stress in the flange-to-skin weld was about 5 ksi. As described in Appendices A and D, the assumptions made for the cycle counts and damping rate were used to compute the magnitude of the decaying load cycles. The stress levels associated with those load cycles were assumed to be linearly proportional to the maximum load.

The peak stresses for the other loading events were computed by linearly scaling the liftoff event peak stress value in proportion to the ratio of the maximum tensile line load of the event to the maximum tensile line load of the liftoff event.

- **F-2 For perfectly planar flanges with ideal contact, the maximum axial stress occurs at the flange-to-skin fillet weld interface with a peak value of approximately 13 ksi for tensile loading and 5.2 ksi for compressive loading.**

7.3.2 Mean Stress

The weld and assembly fit-up generate residual stresses that were assumed to be constant in the circumferential direction and independent of crack growth. The combined residual stresses were treated as a mean stress that elevated or lowered the mean values of all stresses, but not the stress ranges, of the cyclic stresses. No other loads, such as the dead load of the assembled vehicle and the loads caused by personnel working on the internal platforms, were considered significant contributors to either the mean or cyclic stresses and hence were neglected in this analysis.

7.3.2.1 Assembly-Induced Stress

The AIX USS common segment manufacturing process inherently resulted in out-of-plane waviness for mating flange pairs. This waviness was primarily caused by weld distortions. At the time of this analysis, the AIX USS Project had not determined the maximum local gap that could exist between adjacent flanges. However, the tolerance had been specified as +/- 0.005 inch, i.e. the gap could be as large as 0.010 inch.

Several finite element analyses were performed to evaluate the stresses caused during assembly, parametrically varying the location and shape of the gap between mating flanges. The analyses indicated that the "worst case" fit-up stresses would be about 20 ksi.

- **F-3 Assembly stresses that develop due to bolting of non-planar mating flange faces, near the fillet flange-to-skin weld are sensitive to initial flange gapping**

distribution and magnitudes. A warpage of the flange surface of 0.005 inch (giving a maximum mismatch of 0.010 inches) can result in fit-up stresses as high as 20 ksi.

At the time of this writing, the AIX USS Project was pursuing a solution that would machine the surfaces flat after the completion of the flange-to-skin weld, reducing the local gap and thereby minimize the stresses resulting from the joint assembly.

7.3.2.2 Weld Residual Stress

The weld process (e.g., weld pass sequence, heat inputs, and material behavior) and the geometry of the AIX USS segment flange-to-skin weld influence the weld residual stresses. The NESC team obtained the weld processes from the AIX USS Project and modeled the AIX USS segment to evaluate the residual stress distribution through the thickness of the skin, as described in Appendix E. The residual stresses in the vicinity of the weld were estimated for the three weld sequences shown in Figure 7.3-1. The location of the last pass had a large influence on the residual stress behavior, as shown in Figure 7.3-2. The weld sequences with the last pass on the OD resulted in compressive residual stresses near the inner diameter (ID) surface and tensile residual stresses near the mid-thickness. In contrast, the weld sequence with the last pass on the ID resulted in tensile residual stresses near the ID surface and compressive residual stresses near the OD surface. The predicted worst-case among the AIX USS design options analyzed by the NESC team (7 passes, last pass on ID) residual stresses and fit-up stresses both had peak values on the ID surface, as shown in Figure 7.3-3.

The AIX USS Project originally considered the 6-pass and 7-pass weld sequences with the last pass on the OD, however, changed to a 7-pass weld sequence with the last pass on the ID for the initial production welds. This resulted in an undesirable condition of coincident peak cyclic and mean stresses on the ID surface. Cracks growing on the ID under these conditions will have lower CIFS values than cracks growing in welds where the peak cyclic stress coincided with compressive residual stresses. The AIX USS Project changed their weld process to always have the last pass on the OD. Thus, some of the AIX USS common segment flange-to-skin welds have the last pass on the ID and others have the last pass on the OD.

- **F-4 The magnitude and distribution of welding residual stresses are extremely sensitive to the welding procedure – that is, weld joint design, welding heat input, welding process, and particularly to weld sequence.**

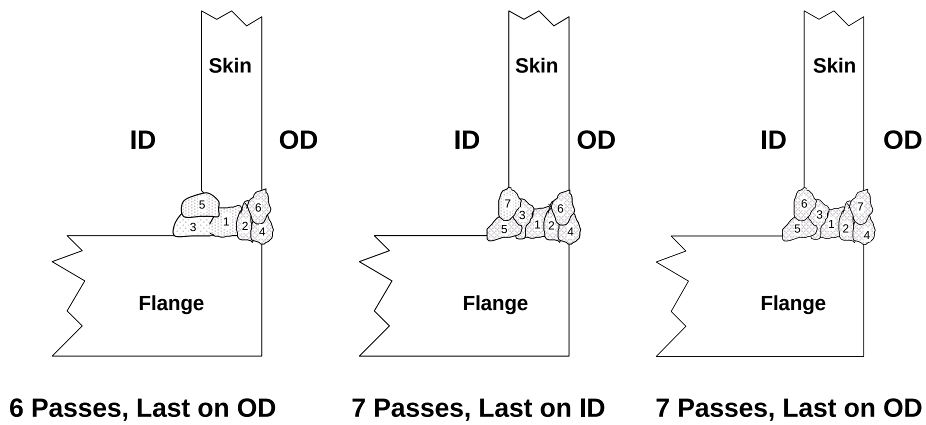

Figure 7.3-1. Weld Sequences Considered in the Residual Stress Analysis

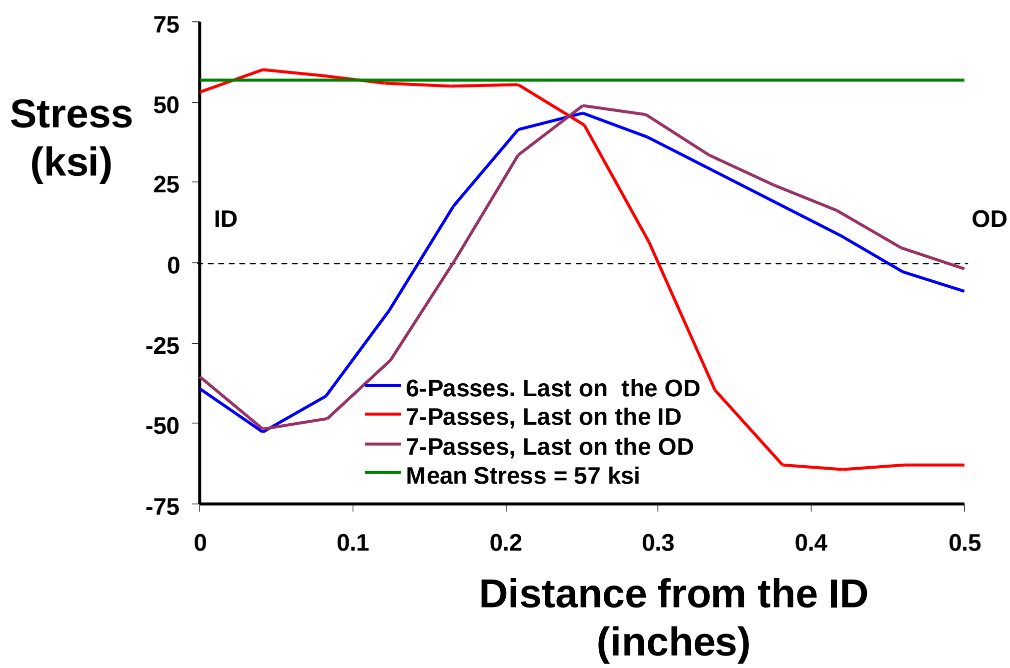

Figure 7.3-2. Distribution of Predicted Residual Stresses for the Weld Sequences Considered in the Residual Stress Analysis

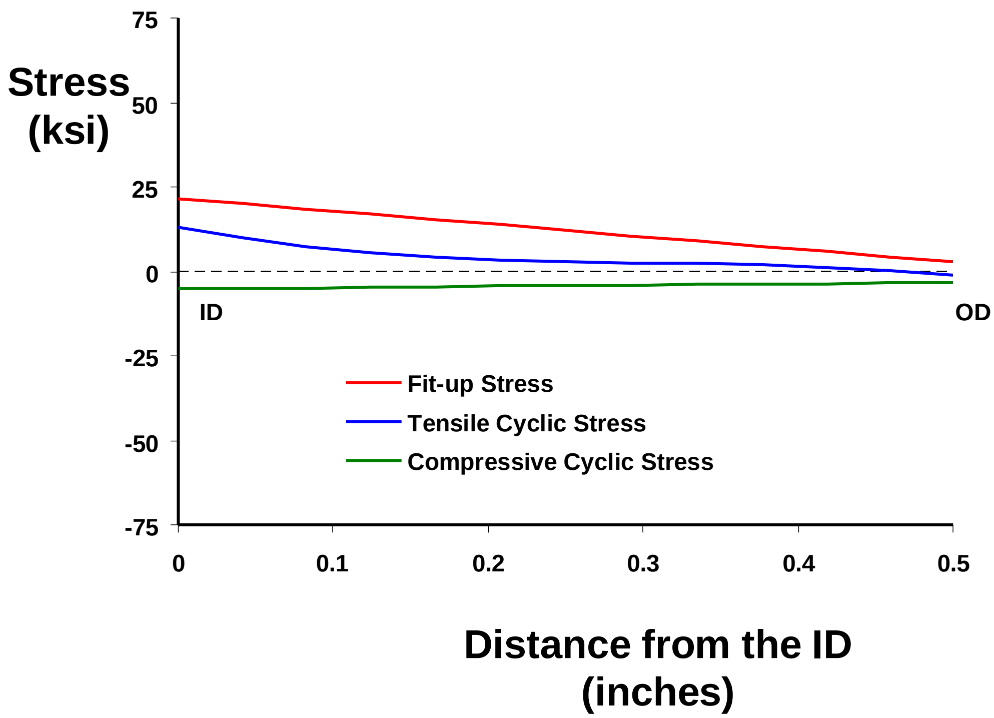

Figure 7.3-3. Distribution of Mean and Peak Cyclic Axial Stresses

7.4 Weld Characterization

Arc welding processes are susceptible to the creation of defects (porosity, crater cracks, lack of fusion, slag inclusions, etc.) near the start/stop regions. These defects can be crack initiation sites and were treated as linear indications in CIFS analyses. Cracks initiating from defects in the weld are influenced by the residual stresses and the fracture toughness behavior of the weld, heat affected zone (HAZ), and the parent materials. Steels are also prone to a sharp reduction in the fracture toughness as the operational temperature decreases below the ductile-to-brittle transition temperature. Testing is required to evaluate weld fracture toughness behavior and weld process controls are required to maintain consistent behavior throughout the entire weld. The AI-X USS Project was developing the weld process as it was undergoing the manufacturing process and several changes occurred throughout the assessment. Therefore, the analysis performed by NESC *may not* represent the final flight weld due to changes that have occurred since the completion of the CIFS analysis.

- **F-5 Arc welding processes are prone to the generation of defects such as porosity, crater cracks, lack of fusion, and slag inclusions at the start stop regions due to inherent arc instability during the transitory operation.**

7.4.1 Weld Properties Evaluation

The CIFS analysis required inputs describing the properties of the parent material as well as the weld material. The parent material has been characterized and limited data was available in the public domain. However, welded joints are highly process dependent and therefore the NESC team conducted testing to determine properties such as fracture toughness, ductile-brittle (Charpy) transition temperature, and fatigue crack growth rates.

The Charpy impact test results on a developmental (non-flight) weld indicated the ductile-to-brittle transition temperature is below -20^o F for the pulse metal inert gas (MIG) weld process. This is below the anticipated minimum exposure temperature of +20^o F (per the AIX USS Fracture Risk Mitigation Plan) to be experienced during assembly, transportation and service.

The ductile-to-brittle transition temperature is less than the lowest anticipated temperature; this does not eliminate the possibility of brittle (cleavage) fracture. An appropriate temperature margin is necessary. The ASME Boiler and Pressure Vessel Code requires that the ductile-to-brittle transition temperature be on the order of 60 ^{o} F, or more, less than the lowest temperature of concern. Another approach is to require that the fracture surfaces of the Charpy-impact specimens contain no flat fracture at some temperature less then the minimum operating temperature.

- **F-6 The Charpy impact test results on a developmental (non-flight) weld indicated the ductile-to-brittle transition temperature is below -20^o F for the pulse MIG weld process**

The initial flange-to-skin weld design and process consisted of a pulsed metal inert gas (MIG) weld of a single bevel joint configuration. During the initial manufacturing evaluation, the AIX USS Project switched to a flux cored arc weld technique and a single-bevel joint configuration. The final weld process selected by the AIX USS Project was a flux cored arc weld technique using a K–bevel or double-bevel joint configuration. Some of the AIX USS production welds had the final pass on the ID and others had the final pass on the OD.

The high ductility of the A516 steel results in a large amount of plastic deformation that precludes any practical calculation of a linear elastic K_{IC} value. Instead, tests were conducted to determine the elastic-plastic J_{IC} value. The fracture tests were conducted on through-the-thickness cracks, while the cracks in the structure were likely to be surface or embedded cracks. These differences in crack configuration may possibly result in different triaxiality stress conditions, or constraint, and fracture toughness values developed from fracture tests conducted on through-the-thickness cracks may not be conservative for surface or embedded cracks. The CIFS analysis used only the elastic component of the measured fracture toughness value to ensure that a conservative value for fracture toughness was used. This assumption was verified to be conservative by the analysis described in Appendix F.

The pulse MIG welding process resulted in an elastic component toughness value of 106 ksi in.$^{1/2}$ based upon a lower bound with a 90 percent confidence using ***six*** samples. The single bevel flux cored welding process resulted in an elastic component of the toughness value of 62 ksi in.$^{1/2}$ from ***three*** samples and the same lower bound confidence. The latter value was used in the NASGRO analysis to predict CIFS. The test procedure and results are presented in Appendix C.

- **O-2 Fracture toughness can be strongly influenced by the weld procedure, such as weld process, sequence, speed, material, and heat input. Also, changes to the weld sequence can result in a marked shift in the location of tensile and compressive residual stresses.**

The current weld process being used on the AIX USS hardware has not been tested for toughness by either the NESC team or the AIX USS Project. The subsequent testing of the current weld process may yield a value that is different from the values sited above, particularly due to the differences in weld process. Also, the 90 percent confidence band on the fracture toughness will increase as the number of samples tested increases if the standard deviation of the sample distribution doesn't substantially increase.

- **F-7 Fracture toughness tests have been conducted on single-beveled pulse MIG welds and single-beveled flux cored welds resulted in different fracture toughness values. No fracture toughness tests have been conducted on the K-beveled flux cored welds in the current baseline manufacturing plan.**

7.4.2 Weld Toughness Control

The NESC acquired the consulting services of Acute Technological Services, a welding engineering firm, to provide expert guidance to the NESC team and to the AIX US Project. Michael Hayes, President of the firm, evaluated the weld procedures as they were being developed by the AIX USS Project and provided guidance in several areas. One of the key findings dealt with the variability of the properties of weld wire. To maintain high consistency in the toughness of the weld, control of the wire properties must be maintained. The most reliable way to achieve consistent toughness value is to acquire all weld wire from the same lot and to control its storage and use.

- **O-3 Historical data have shown that lot-to-lot variability of flux cored wire has a significant influence on the fracture toughness of welds.**

This variability has been attributed to differences in core constituent mixing and blending operations where some metallic components of the flux cored wire becomes segregated due to density differences and the wire becomes enriched along some portion of its length and low in alloying additions in other regions. This may cause inconsistent weld metal microstructures and consequently varying mechanical properties. This characteristic of flux and metal cored welding wire has been recognized for many years and for fracture critical applications many end users require batch or heat testing for all wire to be used.

7.5 Critical Initial Flaw Size Prediction

A CIFS analysis was conducted on the flange-to-skin weld of the AIX USS common segments. The analysis used LEFM assumptions to predict the fatigue crack growth rate of surface and embedded cracks at the ID and OD surfaces of the weld. The analyses used a number of assumptions, the majority of which were conservative, to account for unknowns and uncertainties. In some cases, assumptions were required that could not be demonstrated to be conservative or were likely to be non-conservative. The non-conservative assumptions were evaluated and considered to have relatively minor impact compared to the conservative assumptions.

A CIFS analysis predicts the crack size versus cycles (a versus N) curve using the material behavior (fatigue crack growth rate and fracture toughness), loading spectrum for the structure, and the stress intensity factor for the crack configuration. The critical flaw size (a_{CFS}) is assumed to occur when the maximum stress intensity factor for any one cycle of the loading spectrum equals the material fracture toughness value. The number of spectrum repeats necessary to grow the crack from a_i to a_c is N_c. The CIFS (a_{CIFS}) is defined for this application as the largest crack length that will survive four repeats of the spectrum, as illustrated in Figure 7.5-1. A CIFS analysis requires the following information:

- Loading spectrum
- Shape and size of the initial crack
- Stress-intensity factor solution

- Material behavior that describes the fatigue crack growth rate
- Material behavior that describes the critical stress-intensity factor (fracture toughness)
- A fatigue crack growth rate code that processes the above information

The details of the definition of the loading spectrum, the stress-intensity factors, and the material behavior are described in Appendix A.

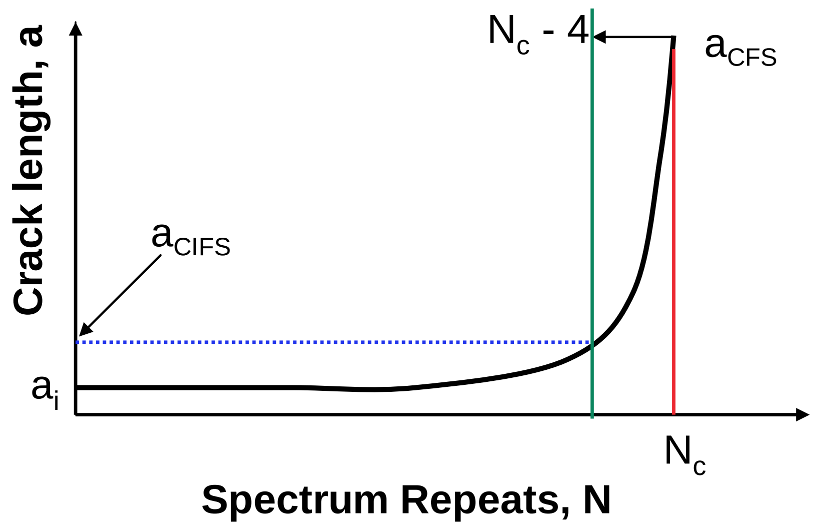

Figure 7.5-1. Repeats of the Spectrum

The CIFS analyses were conducted using the NASGRO fatigue life code. The analysis considered long surface and embedded cracks and determined the combination of crack length and depth that would grow to a critical value in four repeats of the spectrum. A plot of the critical crack depth as a function of the critical crack length indicates the safe and non-safe combinations of crack length and depth, as illustrated in Figure 7.5-2.

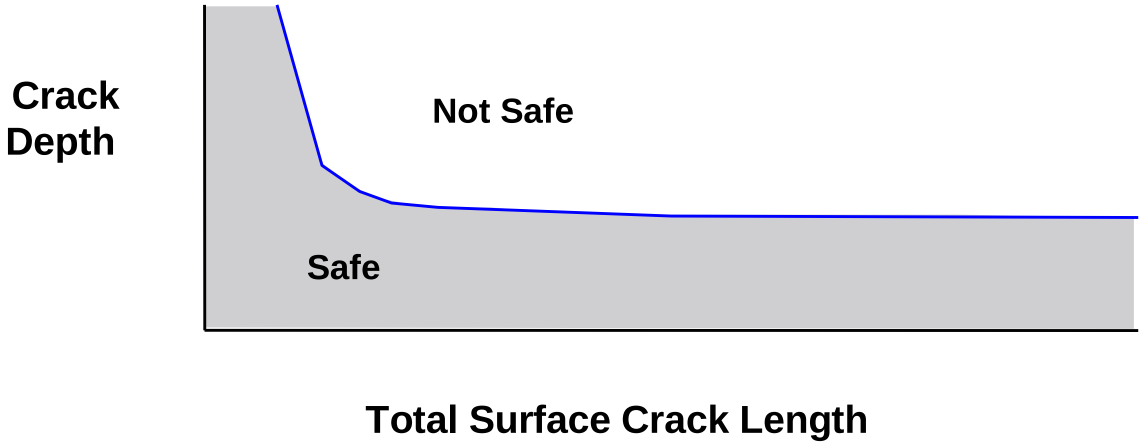

Figure 7.5-2. Results Identify Safe and Unsafe Regions of Crack Size (as well as Crack Shape, Which is Characterized by the Ratio of Crack Depth (a) to Half-Crack Length (c) Such That a/c = 1 Indicates a Semi-Circular Surface Crack)

7.5.1 Parametric Analysis Approach

While the initial objective of this assessment was to determine a single value of a CIFS for the AIX USS Project, it proved more prudent to evaluate a range of crack shapes and configurations (surface versus embedded), as well as local stresses. A parametric analysis was used to illustrate the sensitivity of the CIFS to the above variables, as well as to bound the solution by recommending the CIFS for what the NESC team deemed as a baseline conservative case. This direction was taken because the AIX USS Project underwent a number of design iterations. Specifically, the welding procedure changed the type of weld process, the weld configuration, and the number and sequence of passes. As discussed previously, these changes could impact the weld residual stress levels and locations, and the fracture toughness properties.

The parametric CIFS scenarios evaluated were based upon the same applied load conditions and material behavior. A fracture toughness value of 62 ksi in^{½} was based upon test results on a similar weld process (flux cored), but a different weld configuration (test: single bevel versus production: K-bevel). The worst-case assembly (fit-up) stresses were also assumed to be present and to influence the mean stresses. The parameters that were varied in the analysis included the location and type of the crack and the weld residual stress assumptions.

Cracks in a welded structure typically initiate from surface or sub-surface defects. A fatigue crack that starts as an embedded defect will transition to a surface flaw when one crack front reaches the critical stress-intensity factor, or grows in stable fashion from an embedded to a surface crack. In the current application, surface cracks will generally transition to a through-the-thickness flaw when the crack depth reaches the critical stress-intensity factor. Both transitions described above are illustrated in Figure 7.5-2. The structure was assumed to fail when the stress-intensity factor of the through-the-thickness crack reaches the critical value governed by the fracture toughness. For all practical AIX USS flange-to-skin welds, the through-the-thickness stress-intensity factor immediately became critical upon the transition from the surface crack configuration to a through-thickness crack. Thus, in effect the fatigue crack growth analysis was terminated when the surface crack stress-intensity factor reached the critical value. The CIFS analysis considered an initial crack of the following configurations and locations in the flange-to-skin weld, which are also illustrated in Figure 7.5-3 and 7.5-4.

- A surface crack at the shell ID
- A surface crack at the shell OD
- An embedded defect midway between the shell ID and OD
- An embedded crack that was offset from the shell mid-thickness

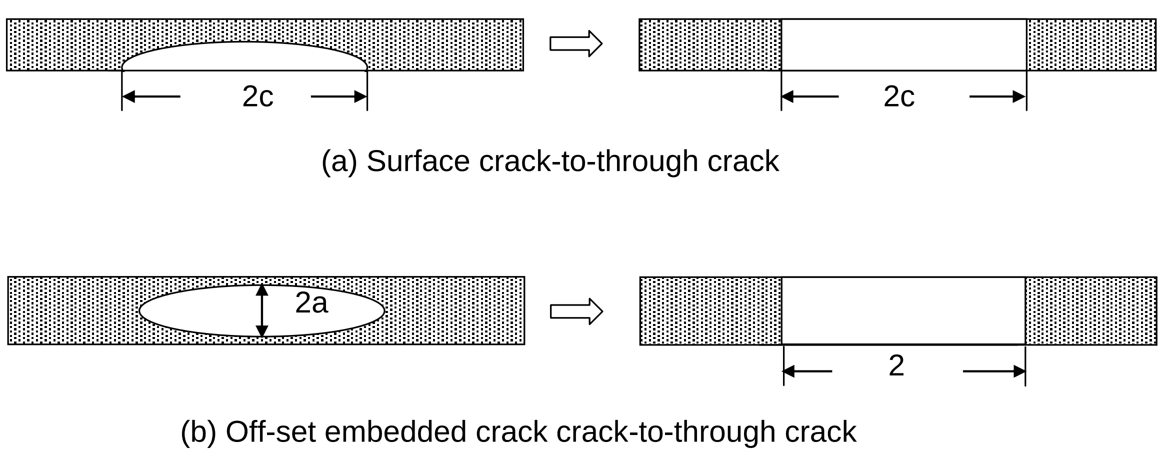

Figure 7.5-3. Surface, Embedded and Through-the-thickness Cracks

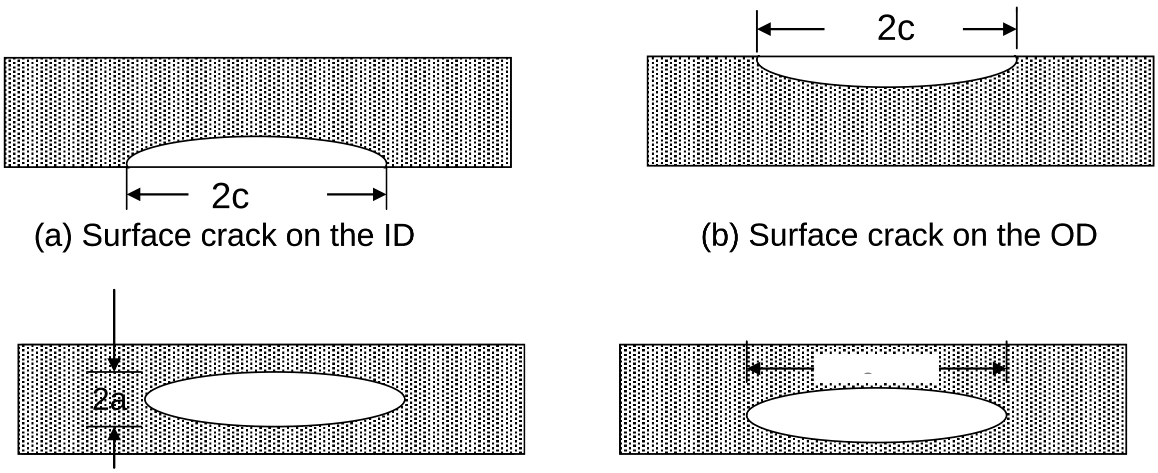

(c) Embedded crack (d) Off-set embedded crack

Figure 7.5-4. Crack Configurations Considered in the CIFS Analysis

The analyses considered four different mean stress cases to account for the weld residual stresses and fit-up stresses:

- Case I - Constant mean stress of the flow stress (57 ksi) to account for the weld residual stresses and fit-up stresses;
- Case II - Residual stresses calculated from a 6-pass weld sequence with the last pass on the OD and the worst case fit-up stresses;
- Case III - Residual stresses calculated from a 7-pass weld sequence with the last pass on the OD and the worst case fit-up stresses; and/or
- Case IV - Residual stresses calculated from a 7-pass weld sequence with the last pass on the ID and the worst case fit-up stresses.

There were several additional parametric analyses that were performed to evaluate the effects of other variables including fracture toughness, assembly stresses and offset amount for an embedded crack. The results of those parametric analyses can be found in the report referenced in Appendix A.

7.5.2 Results Summary

The CIFS results for each of the mean stress assumptions are summarized in Table 7.5-1 and shown in Figure 7.5-5. The assumption of the mean stress equal to the flow stress (57 ksi) provided the lowest bound on the CIFS for all cases except Case IV. This case had the lowest calculated CIFS value of 0.084 inches. Case IV results in high tensile residual stresses on the ID surface. This is the same location that experiences the peak fit-up and cyclic stresses. Neglecting the compressive components of the weld residual stresses had no influence on the CIFS for five of the eight combinations of crack location and mean stress assumption and provided a lower CIFS for the other three combinations. The CIFS for surface cracks was lower than that for embedded cracks for each mean stress assumption examined.

- **F-8 The CIFS was computed using LEFM together with conservative loads, stress-intensity factors, and fracture toughness. The surface crack CIFS value was found to be smaller than that for embedded cracks.**

- **F-9 The weld sequences with the last pass on the OD resulted in compressive residual stresses on the ID surface and larger CIFS values.**

- **F-10 The smallest CIFS predicted for the production AIX USS common segments was 0.084 inches.**

Table 7.5-1. Summary of CIFS Parametric Results

Crack Location	Residual Stress Assumption	CIFS Results (inch)
Surface ID	Mean Stress = Flow Stress	0.116
	6-Pass, Last on OD	0.218
	6-Pass, Last on OD, Pos RS	0.178
	7-Pass, Last on OD	0.25
	7-Pass, Last on OD, Pos Rs	0.186
	7-Pass, Last on ID	0.084
	7-Pass, Last on ID, Pos Rs	0.084
Surface OD	Mean Stress = Flow Stress	0.139
	6-Pass, Last on OD	0.233
	6-Pass, Last on OD, Pos RS	0.233
	7-Pass, Last on OD	0.219
	7-Pass, Last on OD, Pos Rs	0.201
	7-Pass, Last on ID	0.5
	7-Pass, Last on ID, Pos Rs	0.26
Centered Embedded	Mean Stress = Flow Stress	0.32
	6-Pass, Last on OD	0.4
	6-Pass, Last on OD, Pos RS	0.398
	7-Pass, Last on OD	0.411
	7-Pass, Last on OD, Pos Rs	0.411
	7-Pass, Last on ID	0.399
	7-Pass, Last on ID, Pos Rs	0.399
0.125" Offset Embedded	Mean Stress = Flow Stress	0.197
	6-Pass, Last on OD	0.4
	6-Pass, Last on OD, Pos RS	0.208
	7-Pass, Last on OD	0.376
	7-Pass, Last on OD, Pos Rs	0.207
	7-Pass, Last on ID	0.168
	7-Pass, Last on ID, Pos Rs	0.168

(red) Indicates lowest CIFS for a given residual stress assumption

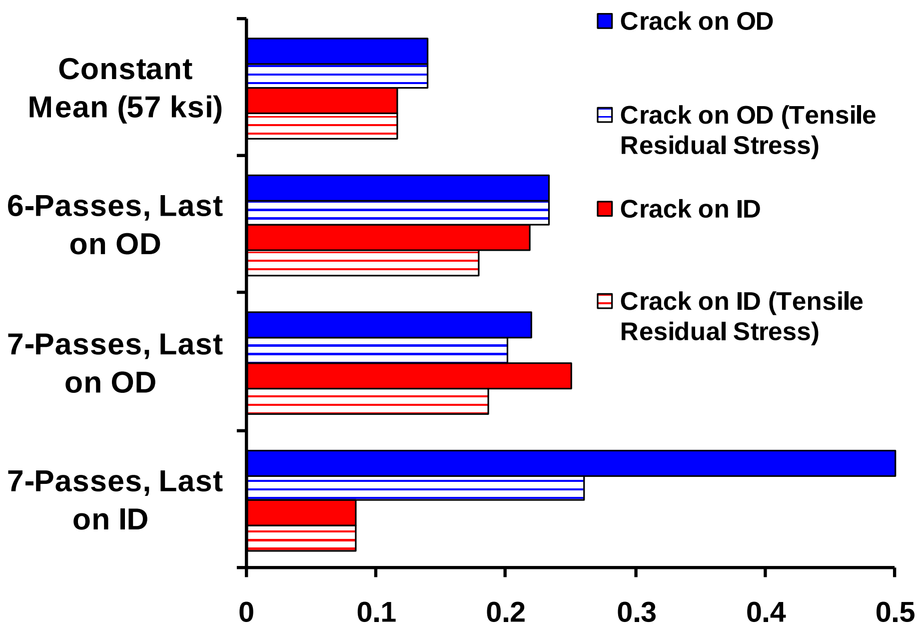

Figure 7.5-5. Summary of the CIFS parametric results

7.5.3 Recommended CIFS for use by AIX USS

The NESC Team results predicted that the smallest CIFS value for the AIX USS production welds was 0.084 inches. This prediction resulted from the lower bound fracture toughness value of 62 ksi inch^{½} and the high tensile weld residual stresses that developed on the ID surface for welds that had the final weld pass deposited on the ID surface. This weld sequence has been used by the AIX USS in the manufacture of several segments of flight hardware. Thus, the CIFS value of 0.084 inches is considered the worst case for the overall AIX USS manufacturing process and is applicable for the current inspection technique pending the results of fracture tests conducted on the flight weld configuration that were recommended by the NESC Team.

The NESC team recommends conducting fracture toughness testing to determine the toughness of the flight weld configurations. From these test results the lower bound value of the fracture toughness with 90 percent confidence can be determined. This lower bound toughness values can be greater than, equal to, or less than 62 ksi inch^{½}. A value that is greater than or equal to 62 ksi inch^{½} would indicate that the current CIFS value of 0.084 inches is conservative, provided all other assumptions are valid (e.g., final coupled loads have been appropriately enveloped) . A value that is less than 62 ksi inch^{½} would require a reexamination of the CIFS analysis using higher fidelity analyses and/or could yield a smaller CIFS which requires a higher resolution inspection technique.

7.5.4 Damage Accumulation

The crack growth damage accumulated for the seven different spectrum loading blocks was characterized using the ID surface crack configuration and the baseline conditions (fracture toughness of 62 ksi inch$^{1/2}$, residual stress distribution, and the worst case assembly stresses), as shown in Figure 7.5-6. Each set of applied loading cycles in a spectrum block is represented by the stress range (ΔS) and the number of applied cycles. The crack growth rate damage (cumulative crack extension) was accumulated for each set of applied cycles and plotted as symbols for damage that exceeds 20, 15, 10, and 5 percent of the total crack growth rate damage. All of the sets of loading cycles that exceeded five percent of the total crack growth rate damage were in the rollout spectrum block. The rollout spectrum block accounted for 96 percent of the crack growth damage. The pad stay and ascent blocks accounted for three percent and one percent of the total damage, respectively. Note that the peak stress that governs the CFS occurs in the liftoff segment, but this segment contains less than one percent of the total crack growth rate damage due to the limited number of cycles present in the block.

- **F-11 The roll out block was the most damaging fatigue component of the spectrum. However, the peak stresses in the lift off block dictate the CFS associated with final fracture.**

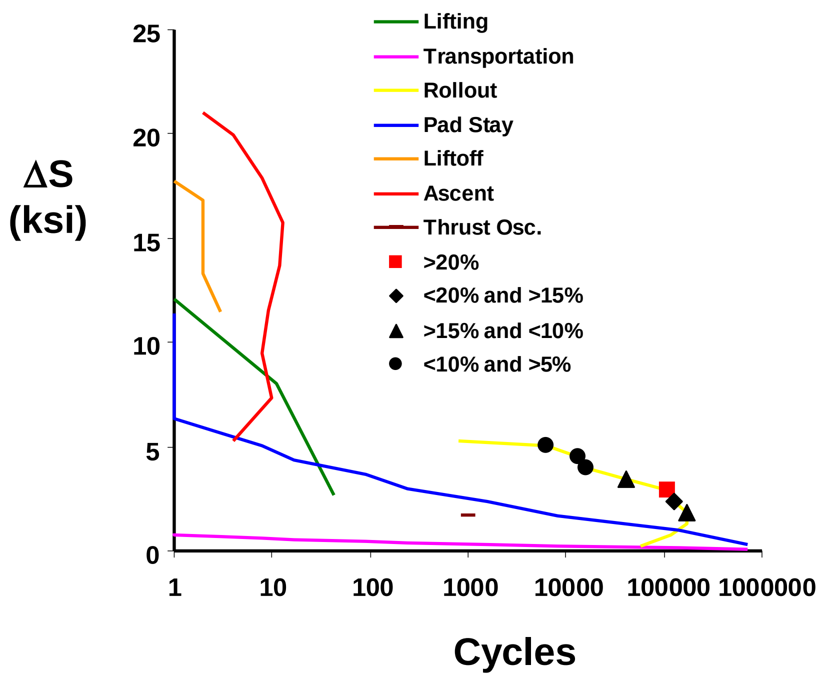

Figure 7.5-6. Crack Growth Damage from Applied Loading Cycles for Each Spectrum Block

7.6 Elastic/Plastic Fracture Mechanics

The CIFS calculations shown previously were made using LEFM, which were considered conservative because they were based on a lower bound, "elastic," fracture toughness determined from tests that displayed significant plasticity. However, there is concern that the residual stresses that were near the magnitude of the yield stresses, when combined with the fit-up and the cyclic stresses, would resulting in conditions that violate LEFM assumptions. Therefore, EPFM analyses were conducted to determine CFS's and these values were compared to CFS values evaluated using LEFM. The approach and results of this study are provided in Appendix F and indicate that using the LEFM approach was conservative for the surface flaw analyses, which were the most critical crack configuration and resulted in the smallest CIFS values.

- **F-12 A higher fidelity EPFM analysis demonstrated that the LEFM assumptions are conservative for the most critical surface flaw configuration.**

7.7 Inspection Procedure Guidance

With appropriate caveats, ultrasound testing (UT) inspection is capable of finding defects significantly smaller than the analytically predicted CIFS values. Based upon NASA-STD (I) 5009, a properly conducted UT inspection is capable of detecting embedded elliptical cracks larger than 0.164 inches by 0.034 inches with a 90 percent probability and a 95 percent confidence level (90/95) in wrought material Cracks of equivalent area, but different aspect ratios (depth/length) are detectable at a similar level.

Based upon the above discussion, the UT method will detect minimum crack areas [(crack depth x crack length) on the order of 0.0055 in^2. This value is to be compared with a minimum predicted CIFS area on the order of 0.021 in^2 (based upon a depth of 0.084 inches and a length of 0.25 inches – the assumed width of the ultrasonic beam). Therefore, a significant difference (4X area) between detectable flaws and the CIFS exists in this application and this provides a substantial margin to allow for uncertainties in the UT measurements due to the complexities of the critical skin-to-flange welds.

- **F-13 The smallest predicted CIFS value is larger than the UT detectable limit, thereby providing margin to allow for uncertainties in NDE measurements due to complexities associated with the AIX USS skin-to-flange weld.**

The AIX USS Project has adopted the AWS D1.1 criteria for screening of flaws. The AIX USS inspection procedure has not been quantified in terms of absolute dimensions of flaws that would be rejected based upon the AWS D1.1 criteria. However, the NESC has assumed that the detectability limit associated with UT in this application is similar to that indicated by NASA STD (I) 5009.

The analysis performed did not evaluate the effects of cracks or defects in close proximity to one another. However, standard practices exist that govern when adjacent crack can be considered a single crack with a length that is the sum of the two crack lengths and the appropriate CIFS assessment made.

- **F-14 CIFS analysis assumes a single flaw (either a surface crack or an embedded crack). Cracks in close proximity to each other may interact, resulting in a longer effective crack length per the guidelines given in API Recommended Practice 579.**

7.8 Conclusion

The NESC team evaluated the CIFS for the AIX USS and found that based upon conservative assumptions, the smallest CIFS value is 0.084 for the US1/US2 interface. The AIX USS selected weld acceptance criteria/standard (AWS D1.1) uses UT inspection for that joint and has sufficient margin on detectability of similar crack areas.

The level of conservatism associated with the fracture toughness value used in the CIFS prediction should be evaluated by the AIX USS Project through testing of flight-like weld coupons. In addition, the future weld joint designs, according to the AIX USS Project will employ a weld sequence that provides a more favorable distribution of the weld residual stress. These factors, if implemented, should provide additional confidence that the CIFS value provided has adequate margin to account for uncertainties in the post-weld UT inspection.

There are some lessons learned from this investigation. While these lessons do not rise to the level of the agency level lessons learned, they may be useful for future investigations and/or for future similar design activities. Therefore, lessons learned from this investigation are presented below.

- Conducting an assessment during the design phase presents a multitude of communication and technical challenges because design details change frequently.
- Before using a new weld process, for which data are not available, determine the weld properties through rigorous testing.
- Welding is a science and the manual or in some cases mechanized application of welding is more of an art. The artistic skill of the welder must be developed over long periods of time and the sourcing and testing of skilled welders is a critical first step for any activity involving large amounts of welding.
- An experienced welding engineer with project ownership responsibility is crucial for activities undertaking extensive welding.
- The Fail-Safe fracture control philosophy is not applicable to welded structures.
- LEFM does not always give conservative results for structures loaded into the elastic plastic regime, even when conservative values of fracture toughness are assumed. This is because the LEFM analysis can significantly underestimate the actual crack driving force under certain conditions; thus, EPFM analyses should be performed to define the limits of the LEFM analysis.

8.0 Findings, Observations, and Recommendations

8.1 Findings

F-1 Peak tension load occurs during liftoff at the US1/US2 interface of 1600 lb/in. (Appendix D)

F-2 For perfectly planar flanges with ideal contact, the maximum axial stress occurs at the flange-to-skin fillet weld interface with a peak value of approximately 13 ksi for tensile loading and 5 ksi for compressive loading. The analysis that generated these predictions was validated by comparison with Single-bolt tests conducted by the AIX USS Project. (Appendix B)

F-3 Assembly stresses that develop due to bolting of non-planar mating flange faces, near the fillet flange-to-skin weld are sensitive to initial flange gapping distribution and magnitudes. A warpage of the flange surface of 0.005 inch (giving a maximum mismatch of 0.010 inches) can result in fit-up stresses as high as 20 ksi. (Section 7.3 and Appendix B)

F-4 The magnitude and distribution of welding residual stresses are sensitive to the welding procedure – particularly weld joint design, welding heat input, weld sequence and welding process. (Appendix E)

F-5 Arc welding processes are prone to the generation of defects such as porosity, crater cracks, lack of fusion, and slag inclusions at the start-stop regions due to inherent arc instability during transitory operation. (Section 7.4)

F-6 The Charpy impact test results on a developmental (non-flight) weld indicated the ductile-to-brittle transition temperature is (below -20^{o} F) for the pulse MIG weld process. (Appendix C)

F-7 Fracture toughness tests conducted on single beveled pulse MIG welds and single beveled flux cored welds gave different fracture toughness values. No fracture toughness tests have been conducted on K-beveled flux cored welds used in the current baseline design. (Appendix C)

F-8 The CIFS was computed using LEFM together with conservative loads, stress-intensity factors, and fracture toughness. The surface crack CIFS value was found to be smaller than that for embedded cracks. (Section 7.5.2 and Appendix A)

F-9 The weld sequences with the last pass on the OD resulted in beneficial compressive residual stresses on the ID surface and larger CIFS values. (Section 7.5)

F-10 The smallest CIFS predicted for the production AIX USS common segments was 0.084 inches. (Section 7.5)

F-11 The roll out block was the most damaging fatigue component of the loading spectrum. However, the peak stresses in the lift off block dictate the CFS associated with final fracture. (Section 7.5.5 and Appendix A)

F-12 A higher fidelity EPFM analysis demonstrated that the LEFM assumptions were conservative for the case of the surface flaw configuration, which gave the smallest CIFS. (Appendix F)

F-13 The smallest predicted CIFS value is larger than the UT detectable limit, thereby providing margin to allow for uncertainties in NDE measurements due to complexities associated with the AIX USS skin-to-flange weld. (Section 7.7)

F-14 CIFS assumes a single flaw (either a surface crack or an embedded crack). Cracks in close proximity to each other may interact, resulting in a longer effective crack length, per guidelines provided in API Recommended Practice 579. (Section 7.7)

8.2 Observations

O-1 Base on available information at the start of this study only the analysis of the flange-to-skin joint of the Common Segments was performed by the NESC team. Other segments may have welds fabricated by other means than the weld that was evaluated and may have higher local stress values (e.g. Interstage Segments).

O-2 Fracture toughness can be strongly influenced by the weld procedure, such as weld process, sequence, speed, material, and heat input. Also, changes to the weld sequence can result in a marked shift in the location of tensile and compressive residual stresses.

0-3 Historical data have shown that lot-to-lot variability of flux cored wire has a significant influence on the fracture toughness of welds. (Section 7.4)

8.3 Recommendations

R-1 Use a CIFS value of 0.084 inches for the US-1/US-2 segment when assessing the effectiveness of post-weld inspection requirements. **[F-12]**

R-2 Consider the uncertainty of the standard UT inspection procedure (NASA-STD-5009) with respect to the predicted CIFS dimensions. **[F-12]**

R–3 Perform a final CIFS analysis for all critical welds (such as the Interstage Segment) based upon the procedures identified in this report using fracture toughness values, welding residual stresses, crack locations, and fit-up stresses based on the final qualified welding and assembly processes. **[F-1 through F-16]**

R-4 Develop, qualify, and maintain consistent weld procedures. **[F-6 and F-9]**

R-5 Procure all the flux core weld wire from the same lot that was used in weld qualification to maintain quality control on the resulting welds and fracture toughness. **[F-9]**

R-6 Conduct an adequate number of J_{IC} tests to characterize the variability for both the HAZ and weld fracture toughness once the weld procedure has been finalized and qualified. **[F-8]**

R-7 Conduct Charpy impact test to verify that the transition temperature is below the anticipated minimum temperature to be experienced during assembly, transportation, and service once the weld procedure has been finalized and qualified. **[F-7]**

R-8 Control flange warpage to minimize the assembly stress levels – that is the total gap between mating flanges prior to bolting should be less than 0.010 inch. **[F-3 and F-4]**

R-9 Perform continuous weld volumetric inspection because of the likely occurrence of intermittent, sub-surface weld defects. **[F-12 and F-16]**

R-10 Pay particular attention to identify and inspect locations of weld starts and stops. **[F-6]**

R-11 Experimentally validate analysis models (e.g. Single-bolt test) used to determine the stresses for CIFS analysis. **[F-1]**

R-12 Assess multiple flaw indications which are in close proximity to one another using API Recommended Practice 579. **[F-16]**

R-13 Design the weld sequences and repairs techniques (if any) to control the magnitude and distribution of weld residual stresses. For all configurations, the final weld pass should be deposited on the OD. **[F-11]**

9.0 Alternate Viewpoints

This section is not applicable; there were no alternate viewpoints or disputed items.

10.0 Other Deliverables

The following deliverables are included within the appropriate appendices. There were no other unique deliverables for this activity.

- A516 Normalized Material properties tests
    - Toughness test results
    - Crack growth rate test results
        - Air environment
        - Salt water environment
    - Charpy impact test results
    - Nil Ductility test results
- Single Bevel Mechanized Weld Procedure
    - Fracture Toughness Test Results
- Single Bevel FCAW Procedure
    - Fracture Toughness Test results

11.0 Lessons Learned

There were no lessons learned to report.

12.0 Definition of Terms

Corrective Actions	Changes to design processes, work instructions, workmanship practices, training, inspections, tests, procedures, specifications, drawings, tools, equipment, facilities, resources, or material that result in preventing, minimizing, or limiting the potential for recurrence of a problem.
Finding	A conclusion based on facts established by the investigating authority.
Lessons Learned	Knowledge or understanding gained by experience. The experience may be positive, as in a successful test or mission, or negative, as in a mishap or failure. A lesson must be significant in that it has real or assumed impact on operations; valid in that it is factually and technically correct; and applicable in that it identifies a specific design, process, or decision that reduces or limits the potential for failures and mishaps, or reinforces a positive result.
Observation	A factor, event, or circumstance identified during the assessment that did not contribute to the problem, but if left uncorrected has the potential to cause a mishap, injury, or increase the severity should a mishap occur. Alternatively, an observation could be a positive acknowledgement of a Center/Program/Project/Organization’s operational structure, tools, and/or support provided.
Problem	The subject of the independent technical assessment/inspection.
Proximate Cause	The event(s) that occurred, including any condition(s) that existed immediately before the undesired outcome, directly resulted in its occurrence and, if eliminated or modified, would have prevented the undesired outcome.
Recommendation	An action identified by the assessment team to correct a root cause or deficiency identified during the investigation. The recommendations may be used by the responsible Center/Program/Project/Organization in the preparation of a corrective action plan.
Root Cause	One of multiple factors (events, conditions, or organizational factors) that contributed to or created the proximate cause and subsequent undesired

	outcome and, if eliminated or modified, would have prevented the undesired outcome. Typically, multiple root causes contribute to an undesired outcome.
Preventive Measure	An action identified by the assessment team to reduce or mitigate the risk of a failure occurring.

13.0 List of Acronyms

ADAC-2	Ares-I Design Analysis Cycle 2
AIX	Ares I-X
AIX USS	Ares I-X Upper Stage Simulator
AVIO	Ares Vehicle Integration Office
AWS	American Weld Society
CIFS	Critical Initial Flaw Size
CFS	Critical Flaw Size
CDR	Critical Design Review
CM	Crew Module
CRT	Crawler Transporter
CT	Compact Tension
EP	Elastic Plastic
EPFM	Elastic Plastic Fracture Mechanics
FCAW	Flux Cored Arc Welding
FM	First Stage
GMAW	Gas Metal Arc Weld
GRC	Glenn Research Center
GTAW	Gas Tungsten Arc Welding
HAZ	Heat Affected Zone
ID	Inner Diameter
JSC	Johnson Space Center
KSC	Kennedy Space Center
LaRC	Langley Research Center
LEFM	Linear Elastic Fracture Mechanics
MIG	Metal Inert Gas
MLP	Mobile Launch Platform
NDE	Non-Destructive Evaluation
OD	Outer Diameter
PGMAW	Pulsed Gas Metal Arc Welding

POD	Probability of Detection
RSRM	Reusable Solid Rocket Motor
RT	Radiography Testing
SRB	Solid Rocket Booster
TDT	Technical Development Teams
USS	Upper Stage Simulator
UT	Ultrasonic
VAB	Vehicle Assembly Building
VFT	Virtual Fabrication Technology

14.0 References

1. Nondestructive Evaluation (NDE) Capabilities Data Book (Third Edition) Published by the Nondestructive Testing Information Analysis Center (NTIAC), Texas Research Institute, Austin TX, Nov. 1997.
2. E-mail notes from the MSFC Fracture Control Board Chairman, Gregg Swanson and the MSFC Damage Tolerance Team Leader, Wayne Gregg on July 31, 2007.

Volume II: Appendices

A Fracture Mechanics Report
B Structural Analysis Report
C Material Testing Report
D Loads Analysis Report
E Residual Stress Report
F Elastic Plastic Fracture Mechanics Report
G Weld Assessment Report
H NDE Report

Technical reports to be formatted in the NASA/SP-1999-7602 style.

- Fracture Mechanics Report (D.Dawicke)
- Structural Analysis Report (N, Knight)
- Material Testing Report (D. Dawicke)
- Loads Analysis Report (C. Larsen)
- Residual Stress Report (Bud Brust)
- Elastic Plastic Fracture Mechanics Report (Steve Hudak)
- Weld Assessment Report (Michael Hayes)
- NDE Report (Sam Russell)

Appendix A. Fracture Mechanics Report

Ares I-X USS Critical Initial Flaw Size (CIFS) Analysis

For usual aerospace applications, the NASA-STD-5001A life requirement is applied to fatigue assessments that only consider notch effects. However, typical fatigue analyses are inadequate to assess life when defects exist such as weld defects. For structures containing welding defects, the fatigue life requirement needs to be addressed by damage tolerance methodology as defined in NASA-STD-5019. (Reference 1)

An independent assessment was conducted to determine the critical initial flaw size (CIFS) for the flange-to-skin weld in the Ares I-X Upper Stage Simulator (USS). The CIFS analysis was conducted to determine the largest crack in the weld region that will not grow to failure within 4 lifetimes. A CIFS analysis assumes an initial crack size (a_i) and grows that crack according to the material behavior (fatigue crack growth rate and fracture toughness), loading spectrum for the structure, and the stress-intensity factor for the crack configuration. The critical flaw size (a_{CFS}) is obtained when the maximum stress-intensity factor for any one cycle of the loading spectrum exceeds the fracture toughness value. The number of spectrum repeats necessary to grow the crack from a_i to a_{CFS} is N_c. The CIFS crack length (a_{CIFS}) is defined as the largest crack length that will survive 4 repeats of the spectrum, as illustrated in Figure A-1. A CIFS analysis requires the following information and additional details are presented in Reference 2:

- Loading spectrum
- Crack shape, size, and the stress-intensity factor solution
- Material behavior that describes the fatigue crack growth rate
- Material behavior (fracture toughness) that determines the critical stress intensity factor
- A fatigue crack growth rate code

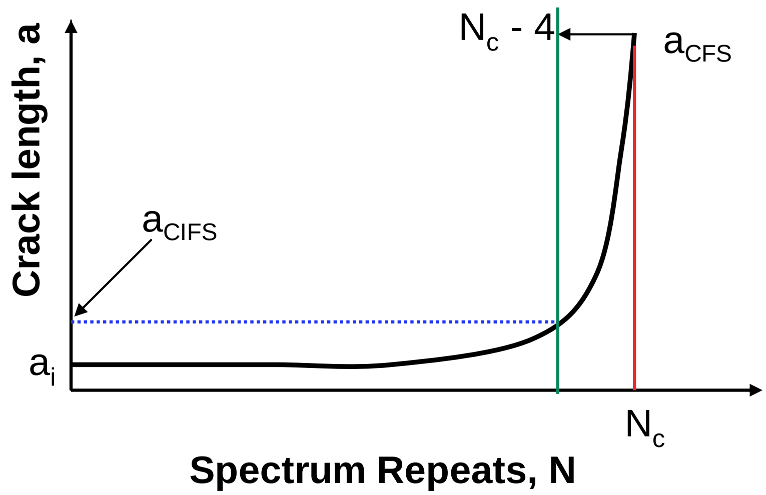

Figure A-1. Schematic of the CIFS approach

The CIFS analysis used linear elastic fracture mechanics assumptions to predict the fatigue crack growth rate of surface and embedded cracks in the inside (ID) and outside (OD) surfaces of the flange-to-skin weld. The analyses used a number of assumptions, the majority of which were conservative, to account for the unknowns and uncertainties of the problem. However, some of these assumptions are not verifiable as conservative as discussed in reference 2. The analyses considered four different mean stress assumptions to account for the weld residual stresses and fit-up stresses:

- Constant mean stress of the flow stress (54 ksi) to account for the weld residual stresses and fit-up stresses
- Residual stresses calculated from a 6-pass weld sequence with the last pass on the ID and the worst case fit-up stresses (largest fit-up stresses calculated with the largest mismatch in the flange flatness)
- Residual stresses calculated from a 7-pass weld sequence with the last pass on the ID and the worst case fit-up stresses
- Residual stresses calculated from a 7-pass weld sequence with the last pass on the OD and the worst case fit-up stresses

The CIFS results for each of the mean stress assumptions are shown in Figure A-2. The assumption of the mean stress equal to the flow stress (54 ksi) provided the lowest bound on the CIFS for all cases except for ID cracks in the 7-pass weld sequence with the last pass on the OD. The 7-pass weld sequence with the last pass on the OD results in high tensile residual stresses on the ID surface. Neglecting the compressive components of the weld residual stresses had no influence on the CIFS for 5 of the 8 combinations of crack location and mean stress assumption and provided a lower CIFS for the other 3 combinations.

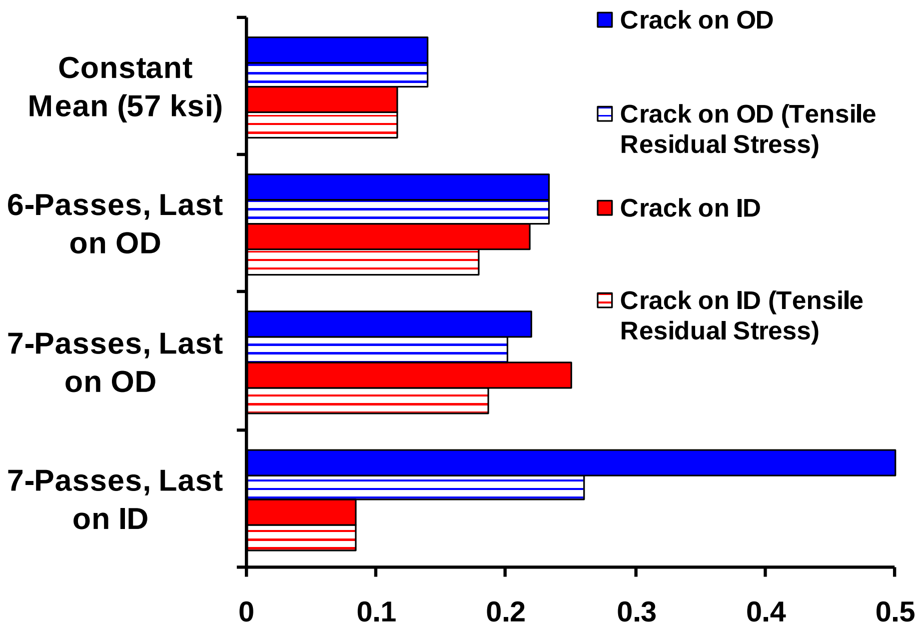

Figure A-2. Summary of the CIFS results

References

1. NASA-STD-5001/5019
2. D. S. Dawicke, I. S. Raju, and D. Cheston "Ares I-X USS Critical Initial Flaw Size Analysis", NASA TM-XXXXX, January 2008.

Appendix B. Structural Analysis Report

Structural Analysis Report

This appendix describes the structural analyses performed supporting the NESC critical initial flaw size assessment of the ARES I-X USS common tuna-can segments. The details of these analyses are presented in Ref [B1].

First, structural analyses of the single-bolt joint configuration were performed to define the modeling and analysis requirements and to calibrate the analysis models against test data. These analyses were elasto-plastic, large-deformation nonlinear finite element analyses. Different parametric studies were performed, and by far, the most significant parameter affecting the single-bolt joint response was the washer-bearing-surface size. Excellent test-analysis correlation (within 5 percent) was obtained for displacements, gap opening, and surface strains, and the results are presented in Ref. [B1].

Next, a repeating unit of the US1/US2 segments, a two segment 10°-wedge, was identified. Finite element models of this 10°-wedge were developed. Structural analysis was performed to examine the stress state in the vicinity of the shell-to-flange weld. Elasto-plastic, large-deformation simulations were performed. The modeling strategy simulated contact conditions along the flange interface between the two segments. Bolt preload was included, and the washer-bearing-surface effects were also simulated using kinematic coupling constraints. The lower edge of the lower segment and the sliced boundaries of both segments had symmetry conditions imposed. The bounding shell in-plane axial tension running load $\tilde{N}_x$ of 1,600 lb/in. was applied to the upper edge of the upper segment.

Since these USS segments are unpressurized and only axial loads are applied in the present CIFS assessment, the radial and hoop components are not anticipated to be significant. The axial stress component is examined for an applied running axial load of 1,600 lb/in., which results in a nominal far-field axial stress of 3.2 ksi. The axial stress varies with location and reaches higher values near each bolt hole and maximum values as the gusset is approached. The axial stress distribution for the perfectly flat flanges is shown in Figure B1 with a maximum axial tensile stress of 12.5 ksi at the top of the fillet weld near the gusset.

Both tensile and compressive applied load cases were analyzed to provide stress data at the top of the fillet weld and the centerline of the gusset and were used as inputs in the fatigue crack growth analyses. The through-the-thickness axial stress distribution for the tension case decreases from the peak tensile value of 12.5 ksi on the inside surface to essentially zero on the outside surface. The through-the-thickness axial stress distribution for the compression case decreases from the peak compressive value given of 5.2 ksi to approximately 3.3 ksi on the outside surface. For the tension case, bending occurs due to the eccentricity of the load path in the joint. For the compression case, bearing occurs due to closing of the joint by the external loading even more than by the bolt preload.

The manufacturing and assembly of large diameter shells and annular ring segments are difficult tasks in terms of maintaining stringent assembly tolerances on flatness, perpendicularity, and parallelism on the mating surfaces. The influence of flange-surface mismatch due to local initial geometric surface imperfections along the flange mating surface contribute to the fit-up stresses. These fit up stresses were evaluated. The peak tensile axial stress at the top of the fillet weld was assessed for the bolt preload step of the structural analysis from a stress free state. The overall axial stress distributions shown in Figure B-1 using a fixed range for the contour intervals were examined for a representative flange mismatch case and the application of the 36,500-lb bolt preload force only. The stress distribution for a periodic mismatch distribution with edge gaps is shown in Figure B-2 with a maximum axial tensile stress of 22.3 ksi. These results indicate that the maximum axial tensile stress at the top of the fillet weld and its circumferential location are dependent on the flange surface mismatch more than the applied external axial loading.

Last, a preliminary assessment of the buckling margins of the US1 segment to dead-weight loading and to in-plane shear (torsional) flight loads. In both loading cases, the US1 segment had high margins against buckling. Details are given in [Ref.B1].

In summary, stress analysis results indicated that the stress levels were well below the material yield stress for the bounding axial tensile design load even with a factor of safety of 1.4. The gussets tend to increase the local stress level near the top of the fillet weld between the gusset and the adjacent bolt hole. Clocking of the gussets during assembly causes only a minor change in the local stress state, and hence, clocking is not an issue. From these structural analyses, for the maximum axial shell running load of 1,600 lb/in. the peak values of the axial stress along the top of the fillet weld at the shell-to-flange interface have been determined to be 12.5 ksi for tensile loading and 5.2 ksi for compressive loading. For a representative flange surface mismatch of 10 mils, the maximum tensile stress was 22.3 ksi. These values are used subsequently in the CIFS analyses.

Reference

B1. Knight, N. F., Jr., Phillips, D. R., and Raju, I. S., *ARES I-X Upper Stage Simulator Structural Analyses Supporting the NESC Critical Initial Flaw Size Assessment*, NASA TM-2008-xxxxxx, 2008.

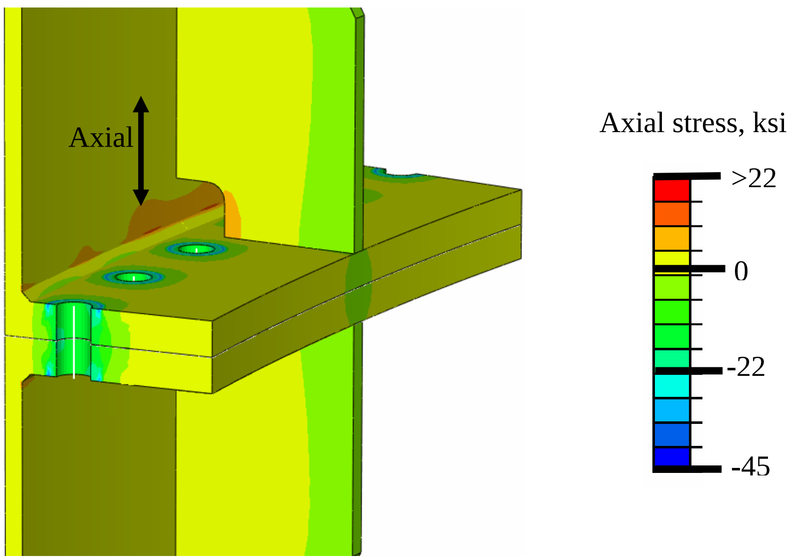

Figure B-1. Axial stress distributions after application of both bolt preload force of 36,500 lb and design axial running load of 1,600 lb/in – assuming perfect flange mating.

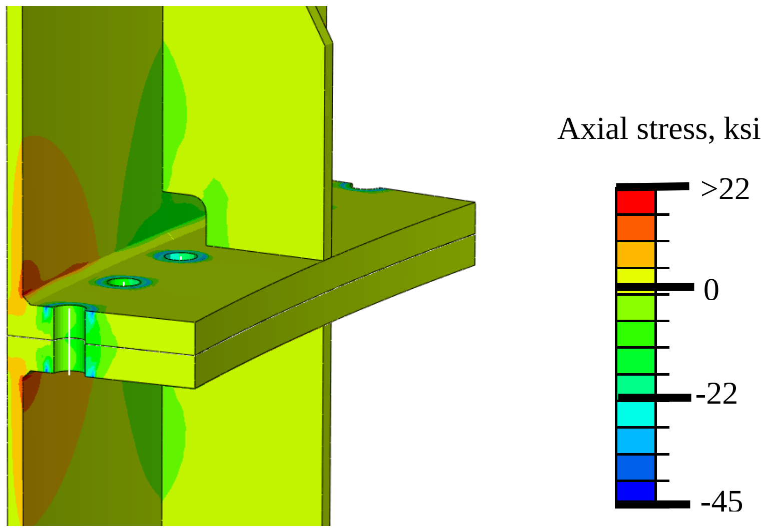

Figure B-2. Axial stress distribution after application of only bolt preload force of 36,500 lb. assuming a 10-mil peak flange mismatch gap midway between two gussets – "fit-up" axial stress distribution.

Appendix C. Material Testing Report

Ares I-X USS Material Testing

An independent assessment was conducted to determine the critical initial flaw size (CIFS) for the flange-to-skin weld in the Ares I-X Upper Stage Simulator (USS). The skin and flange are made of A516 steel and the flange-to-skin weld was initially performed using a pulse MIG process, but the process was changed to a flux-cored welding process for the final production of the USS. Tests were conducted to evaluate the material behavior of the A516 steel with particular attention to the material behavior that could be influenced by the weld process. The types of tests that were run include fatigue crack growth rate in lab air and in a salt-water environment, Charpy impact tests, and fracture toughness tests. Parent A516 material was used for the fatigue crack growth rate tests and plates of welded material were used for the Charpy impact (flux-cored process) and fracture toughness (both flux cored and pulse MIG processes) tests. A summary of the testing results is presented in Table C-1. Additional details on the testing are provided in Reference 1.

Table C-1.Testing Summary

Test Type	Result
Fatigue Crack Growth (Lab Air)	The test results agreed with data from the literature for A516 steel. The following NASGRO equation parameters were used to describe the fatigue crack growth behavior: p = q = 0 c = 6E-10 n = 2.8
Fatigue Crack Growth (Salt Water Environment)	No significant acceleration of the fatigue crack growth rate behavior was observed. The lack of acceleration may be due to corrosion byproduct induced fatigue crack closure.
Charpy Impact Tests	No significant drop in fracture energy was observed for tests conducted in the range of 190^{o}F to –20^{o}F.
Fracture Toughness Tests	The elastic component of the J_{IC} was used to characterize the fracture toughness of the A516 steel. The 0.1/90% lower bound on the fracture toughness 62 ksi inch $^{1/2}$

References

1. D. S. Dawicke, S. A. Smith, and I. S. Raju "Ares I-X USS Material Testing", NASA TM-XXXXX, January 2008.

Appendix D. Loads Analysis Report

At the onset of the NESC assessment, a complete design set of prelaunch, liftoff and ascent loads did not exist for the Ares I-X vehicle. It was mutually agreed by the Ares I-X Upper Stage Simulator Project and the NESC team that a consistent set of load spectra would be used by both teams for their otherwise independent life analyses. Therefore, the NESC team worked in partnership with the loads and dynamics engineers in the Ares I-X Vehicle Integration Office, the Constellation Program Ares I Loads Panel, and the structures team of the Ares I-X USS Project office to develop a set of bounding loads spectra expressly for the purpose of application to the fracture mechanics modeling for the CIFS prediction.

The most comprehensive set of design loads existing at the time were the so-called "mini-loads cycle" results for the Ares I vehicle documented in the MSFC Engineering memo EV30-07-001 "Preliminary Design Loads for Ares-I Design Analysis Cycle 2 (ADAC-2)". The loads provided by this memo resulted from response analyses of pre-launch (pad stay winds), liftoff and ascent flight design environments. Because the design of the Ares I and Ares I-X vehicles did not precisely match, the NESC used the available finite element model geometries of the Ares I-X and Ares I vehicles to interpolate these Ares I loads for the Ares I-X Upper Stage Simulator joint locations.

As the “mini-loads cycle” results were intended for structural strength design purposes, no detailed time history response data were available to perform cycle identification to establish load cycle counts for the CIFS analysis. The team used available environmental data (measured wind speed distributions) or engineering knowledge of the fundamental dynamic response of the launch vehicle to attempt to produce a bounding load spectra for each of the flight regimes discussed below.

Specific flight regimes and pre-launch load conditions considered were: rollout from the VAB to the launch pad, pre-launch pad stay, liftoff, ascent flight, as well as ground handling (crane lifting) and transportation.

Roll-Out from VAB to Launch Pad

The Ares I-X Systems Requirements Document allows for a maximum of five round trips of the AI-X vehicle between the Vehicle Assembly Building (VAB) and the launch pad. The AI-X vehicle will be stacked on a Mobile Launch Platform (MLP) used for Space Shuttle Program and moved by the crawler transporter (CRT). No analytical modeling had been performed by the AI-X project to predict the loads imparted to the AIX specific configuration during this transport, so an assessment was performed by the NESC.
The Ares I-X vehicle was assumed to be supported only at the base, the SRB aft skirt to MLP interface, during transportation from the VAB to the launch complex. At the time of the analysis, no supplemental support system had been defined by the AI-X Project to reduce vehicle stack response due to winds or rollout.

The team commissioned the Loads and Structural Dynamics Branch at the Johnson Space Center (JSC) to perform a forced response analysis using an available NASTRAN model of the Ares I vehicle coupled with a model of the MLP and CT available from the Space Shuttle Program. The Ares I model weight was adjusted to include a fully fueled second stage, which most closely approximated the rollout configuration of the Ares I-X vehicle. Two basic forcing function sets were applied to the NASTRAN model as derived from existing measured response data obtained during roll-out testing performed by the Space Shuttle Program: the first set was derived from response data taken during a “partial stack” Shuttle rollout test that consisted of two Shuttle SRBs mounted on a MLP and connected at their ET forward attach points by an ET cross beam that is normally an internal component of the ET intertank; the second forcing function set was derived from response data taken during the rollout of the STS-115 vehicle, a so-called “full stack” set of data . The CT is normally operated up to a speed of 1.0 mph, and forcing functions were available from the Space Shuttle Program at 0.5, 0.6, 0.7, 0.8, 0.9 mph for the “partial stack” data and at 0.8, 0.9, 1.0 mph for the “full stack” data.

The 0.8 mph “partial stack” forcing function applied to the Ares-I model yielded the highest transverse moment response near the base of what would be the USS due to a near-resonant condition with the 2nd and 3rd bending modes of the vehicle and MLP/CT stack. At a crawler speed of 0.7 or 0.9 mph, the moment response decreased by 50 percent or more. It was decided that both the 0.7 and 0.8 mph responses would be retained to provide sensitivity data should the resulting CIFS analysis prove to be dominated by the rollout environment. The moment responses of both the 0.7 and 0.8 mph speeds were processed through a rainflow cycle identification algorithm to determine the distribution of cycles shown in Table D-1 for one simulated 8-hour trip to the pad from the VAB. In the subsequent CIFS analysis, only the 0.8 mph data was used to provide an upper-bound assessment.

Table D-1. Rollout Speed versus Moment Cycles

Rollout, 8-hours VAB to pad		
	Number of Cycles	
% of Design Moment	0.7 mph	0.8 mph
5%	11160	5256
15%	15048	10584
25%	14688	15768
35%	14256	15840
45%	10296	11592
55%	5904	9936
65%	3240	3744
75%	2232	1440
85%	1800	1224
95%	504	576
100%	72	72
total =	79200	76032

Pad Stay

The Systems Requirements Document requires the Ares I-X vehicle to be designed for a 50 day stay at the launch pad. The NESC assumed a cumulative 300 day stay based upon the previously mentioned requirement of five round trips to the pad, plus one final stay for the eventual launch. The loads acting on the vehicle during this phase of the life cycle are wind and gravity, thus the bending moment which drives any tensile loading in the vehicle joints is proportional to the wind loading (or the square of the wind speed). The Constellation Program Design Specification for Natural Environments (DSNE, CxP 70023) provides the frequency of occurrence distribution for the number of occurrences of peak wind speeds that was used to determine the number of peak wind occurrences in the 300 day period.

At the time of this assessment, both the Ares I and Ares I-X vehicles had been assessed for peak winds corresponding to a 1 percent risk of exceedance for a 10-day pad stay, that is, a peak wind speed of 29.6 meters/second (57.5 knots) at the 18.3 meter reference level for KSC. This was the reference wind speed used to scale the Ares I "mini-loads cycle" pad stay loads to develop the pad winds spectra provided in Table D-2. However, Constellation Program requirements also impose a 38.3 meter/second design wind that must be included as at least one occurrence in any fatigue life assessments. The bending moment from the design peak wind speed of 29.6 meters/second was thus scaled by square of the velocity ratio and a single cycle was added for this condition in the CIFS analysis. The wind loads were all applied as fully reversed cycles in the CIFS analysis, as yet a further upper-bound assumption.

Table D-2.Wind Loading Distribution

Prelaunch wind			
	Number of Cycles		
% of Design Moment	50-day pad stay	6x50-day pad stay	300-day pad stay
5%	118474	710,844	710,843
15%	23729	142,374	142,371
25%	1383	8,298	8,299
35%	260	1,560	1,562
45%	40	240	242
55%	15	90	89
65%	3	18	17
75%	0	0	8
85%	0	0	3
95%	0	0	1
100%	1	1	1
	Total =	863,425	863,437

Liftoff

The liftoff event was assumed to occur over 10-second duration and was assumed to excite the vehicle in free vibration in its first mode of 1 Hz. The cyclic loads experienced during this phase of the life cycle were estimated by approximating the vehicle response as the initial peak load of the liftoff design moment followed by a sinusoidal decay at 1 Hz and 1 percent damping, as shown in Figure D-1.

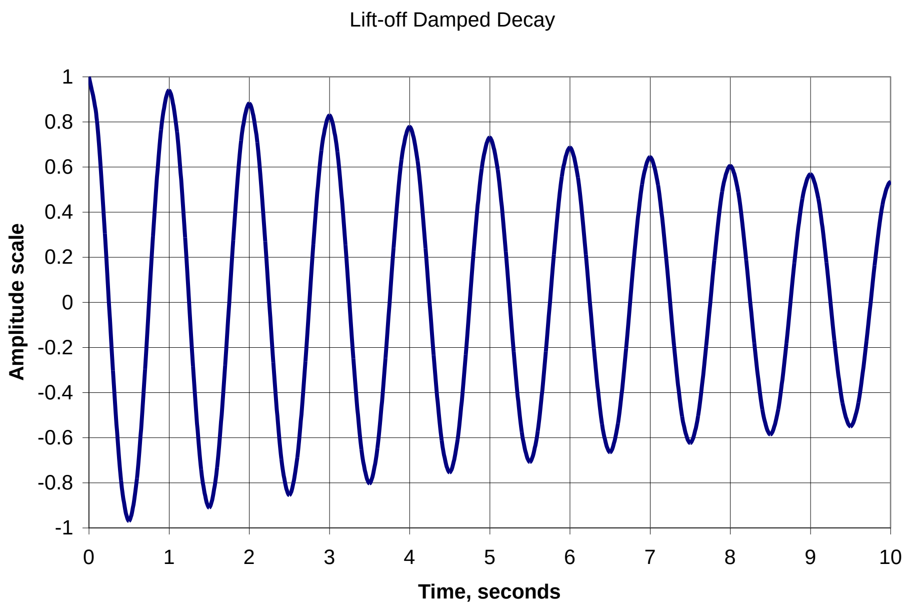

Figure D-1. Liftoff Damped Decay

Ascent

The duration of the powered ascent phase the of Ares I-X flight is approximately 120 seconds, as determined by burn-out of the Space Shuttle SRB used as the first stage. However, for this analysis a 70 second period of significant dynamic pressure (Q > ~350 psi) was determined from examination a typical Ares I planned ascent trajectory. The maximum ascent bending moment from the Ares I mini-loads cycle was assumed to occur at the time of maximum dynamic pressure. A series of ten equally timed ascent loads events was assumed to occur in this 70 second period as an approximation to a series of gust load events. The bending moment at each event time was scaled in proportion to the ratio of Q at that time to Q_{max}. The bending moment for each of the 10 “gust” events was assumed to decay in the seven second interval as a free vibration at 1 Hz with a 1 percent damping rate, as shown in Figure D-2.

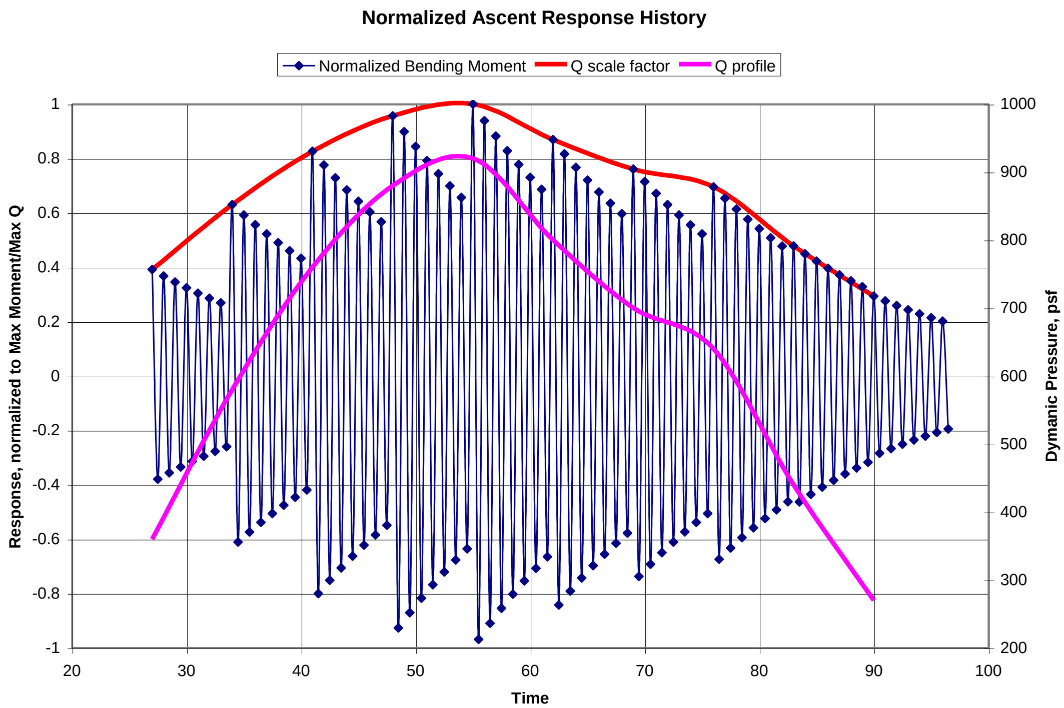

Figure D-2. Normalized Ascent Response History

Ground handling and Transportation Loads

Each segment of the Ares I-X hardware is manufactured separately and is lifted and transported locally several times during assembly. The team assumed that the lifting event consisted of a single 1.5 proof load, 11 multi-segment lifts, and 42 single segment lifts. The transportation event consists of peak loads estimated for shipboard travel. The number of cycles and decay of the shipboard loads were derived from the characteristics of a 50-day pad stay. This assumption was made in the absence of actual transportation data and is believed to be conservative.

Appendix E. Residual Stress Report

Ares I-X USS Residual Stress Analysis Report

The tuna can segment of the ARES upper stage weld was modeled in order to obtain the residual stresses caused by the shell to flange weld. These residual stresses are used in the fatigue and fracture mechanics assessments. Several weld sequences are considered and the importance of weld sequence in controlling residual stresses is illustrated. Finally, a few sensitivity studies are presented which illustrate the effect the weld process on residual stress as well as ‘shake-down’ effects during service loading.

Computational weld modeling is challenging because many of the processes of welding are highly nonlinear. Material melts and re-solidifies, very high transient thermal gradients are experienced, non-linear temperature dependent plastic straining and phase transformations can occur, among other sources of nonlinearity. The weld modeling code, Virtual Fabrication Technology (VFT^{TM}), was used here to predict the flange to shell weld residual stresses. VFT is discussed in detail in Reference 1 and the many references sited therein. There was not direct validation of the model for the flange to shell weld discussed here. However, extensive validation of the computational weld model is available in Reference 2 for weld temperature predictions versus time, distortion predictions, and weld residual stresses so that predictions are presented here with confidence in their accuracy.

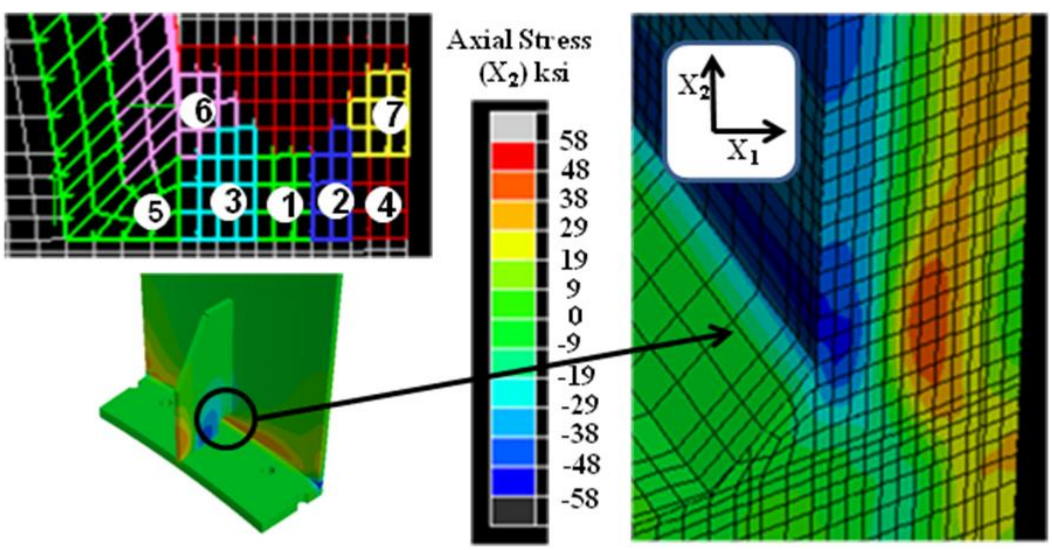

Figure E-1. Weld Residual Stresses for Seven Pass Balanced Sequence Final Pass on OD

A large number of weld sequences, weld parameters, and weld geometries were investigated. Each weld pass is modeled by using a moving heat source as the weld is deposited. A ten-degree segment was modeled with appropriate boundary conditions as discussed in Reference 2. The final sequence suggested by the team is shown in Figure E-1 in the upper left inset. It is seen that a 7 pass balanced weld sequence with the final pass deposited on the OD is the optimum since it induces compressive axial residual stresses on the ID at the toe of the weld (Figure 1). The location at the toe of the fillet at the mouse hole location (lower left inset, Figure 1) was determined to be the critical CIFS location. Circumferential cracks, driven by axial stresses are the controlling crack growth situation here since they combine unfavorably with service loads.

Figure E-2 illustrates the residual stress patterns through the shell wall at the toe of the fillet that was used for the CIFS analysis. The results with the final pass applied to the ID, which reverses passes 6 and 7 in the upper left inset in Figure E-1, shows high tensile ID stresses. These stresses were conservatively used in the CIFS analysis even though an analysis shows that 'shakedown' occurs after the application of the first service load. Shakedown reduces the stresses in Figure E-2.

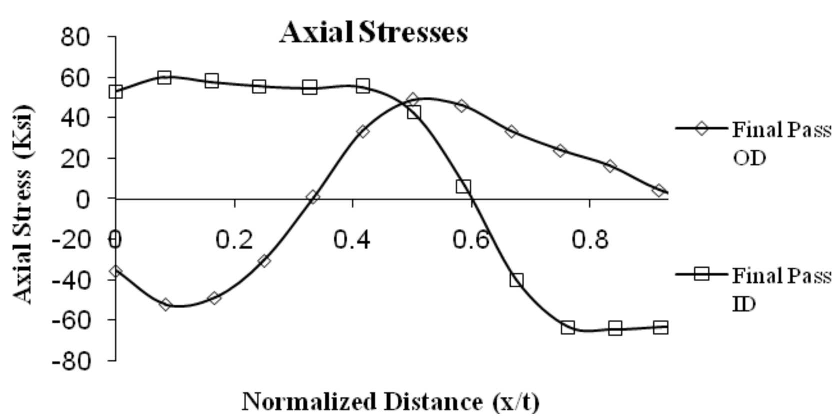

Figure F-2. Axial Stresses through Shell Wall at Top of Fillet

The residual stresses are strongly affected by pass sequence. The mechanism for this behavior is discussed in Reference 2 along with many more details. The final weld residual stress pattern for the ARES shell to flange weld is the result of the competition between axial shrinkage of the weld bead, which produces tension at the final weld location, and radial shrinkage of the bead, which tends to produce tension on the ID and compression on the OD (analogous to shrink fitting a ring on a tube). The thick stiff ring and the gusset stiffener also complicate the final residual stress patterns.

References

1. Brust, F. W., and Kim, D., "Mitigating Welding Residual Stress and Distortion", Chapter 8 in *Processes and Mechanisms of Welding Residual Stress and Distortion,* pp. 264 – 294, Woodhead Publishing, July 2005.
2. F. W. Brust, I. S. Raju, and D. Cheston "Ares I-X USS Weld Residual Stress Analysis", NASA TM-XXXXX, January 2008.

Appendix F. Elastic Plastic Fracture Mechanics Report

Critical Flaw Size Analysis Based on Elastic-Plastic Fracture Mechanics

Independent critical flaw size calculations (CFS) for weld flaws in the flange-to-skin weld of the ARES I-X Upper Stage Simulator (USS) have been reported in Appendix A. These calculations were made using linear elastic fracture mechanics (LEFM). Although the LEFM CFS evaluations are considered conservative because they are based on a lower bound, so-called "elastic," fracture toughness determined from tests that displayed significant plasticity, there is still concern that the yield magnitude stresses generated in the flange-to-skin weld by the combination of axial stresses due to axial forces, fit-up stresses, and weld residual stresses, could give rise to significant crack-tip plasticity and a corresponding increase in the calculated crack-tip driving force that could more than compensate for the conservatisms built into the LEFM approach.

A series of CFS computations were performed using an R&D version of the elastic-plastic fracture mechanics (EPFM) computer program FlawPRO™ developed by Southwest Research Institute for structural integrity assessments of welded pipe in the offshore oil and gas industry. These calculations were made in order to demonstrate that the elastic approach adopted in Appendix A is conservative with respect to a more complex but technically more rigorous and consistent approach based on EPFM. This demonstration is necessary because although the elastic approach uses an "elastic" toughness which is significantly below the measured toughness (62 ksi inch$^{1/2}$ compared to 154 ksi inch$^{1/2}$) it is known that LEFM can under-predict crack-tip driving forces compared to more accurate values determined using EPFM. Under certain conditions, it is possible that the under-prediction of the crack-tip driving force based on LEFM analysis can more than compensate for the use of a low "elastic" toughness, thereby resulting in a non-conservative CFS value.

The CFS computations were made for surface and embedded cracks either at or near to the ID or OD of the flange-to-skin weld in A516 steel. Analyses were performed with axial and fit-up stresses superposed on four types of residual stresses. Unlike the elastic calculations, the elastic-plastic approach requires the applied stresses to be resolved into primary and secondary (residual stress) components. The weld residual stresses considered in the present assessment are:

- A uniform stress equal to the yield stress

- A stress consistent with a double V weld process
- A stress consistent with a 7 pass weld procedure with the last pass on the ID
- A stress consistent with a 7 pass weld procedure with the last pass on the OD

CFS computations using the elastic and elastic-plastic approaches showed that the predicted CFS for surface cracks were significantly smaller than the CFS for embedded cracks. These computations also showed that the uniform and 7 pass (ID last) residual stresses were the most onerous of the four and resulted in the smallest CFS values. These stresses are so severe that when they are combined with those due to axial and fit-up stresses the resulting through-wall stresses exceed the yield stress. In actuality, plastic relaxation of stresses that exceed yield will occur, resulting in so-called shakedown and a reduction in the residual stresses. This shakedown phenomenon can be allowed for in elastic-plastic computations performed by FlawPRO. Shakedown is assumed not to occur in the elastic approach.

A summary of the CCS results for surface cracks is shown in Figure F-1. Additional details on the analysis methods and further discussions of the results are provided in Ref [F1].

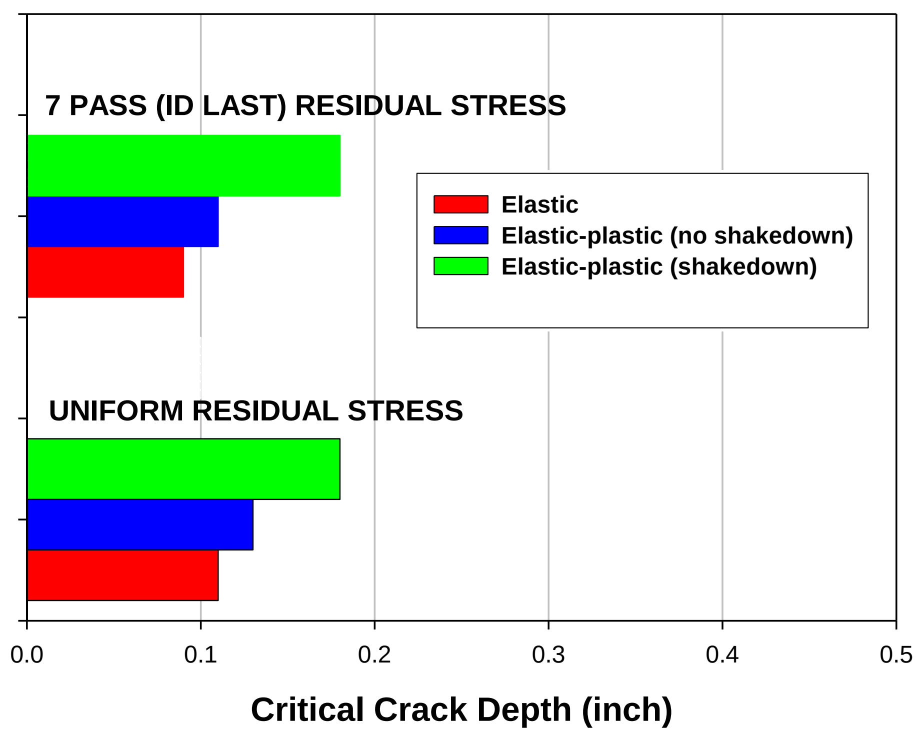

Figure F-1. Summary of CFS values for surface cracks determined using elastic and elastic-plastic approaches, the latter with and without shakedown in residual stresses

It is concluded from Figure F-1 that CFS calculated for the most critical case of surface cracks using an the elastic approach and a toughness of 62 ksi inch$^{1/2}$ will be smaller, and hence more conservative, than values computed using an elastic-plastic approach based on a toughness of 154 ksi inch$^{1/2}$, even if the potentially beneficial phenomenon of stress relaxation from shakedown is ignored. The same is not always true for embedded cracks; however, these cases give larger computed CFCS values than for surface cracks using both elastic and elastic-plastic analyses, and thus are of less concern provided the surface flaw critical initial flaw size (CIFS) results are used to set weld defect acceptance limits.

Reference

F1. Chell, G. Graham, and Hudak, Jr., Stephen J., "Elastic-Plastic Fracture Mechanics Analysis of Critical Flaw Size in Ares1-X Flange-to-Skin Welds, NASA TM-2008-XXXXX, January 2008.

Appendix G. Evaluation of Welding Procedures for Ares USS

At the request of NASA Glenn NESC engineering staff ATS Sr. Welding Engineer Michael Hayes visited the Glenn Research Center in Cleveland to meet with key fabrication and NESC team members as well as outside consultants to review fabrication procedures for the Ares USS modules. The first visit included a tour of the fabrication facility and opportunities to speak with welding technicians and engineers. The following were the primary preliminary conclusions regarding the USS fabrication:

1. The pulsed gas metal arc welding (PGMAW) process was initially being used for the skin long seam welds and was being qualified. The use of the pulsed gas metal arc welding process for the skin welds as well as the flange to skin weld may lead to unacceptable defects of the lack-of-fusion type which are primarily detected by ultrasonic testing with shear wave probes or a combination of shear wave and compression waves. It may be beneficial to consider the use of automated ultrasonic testing for inspection of the skin to flange welds.

2. The importance of locating skilled welders for the pulsed gas metal arc welding process was highlighted and it was reported that an outside contractor has been tasked with supplying skilled craftsman. There are few skilled PGMAW welders available for contract work.

3. Welds with straight sided heat affected zones (HAZ) should be produced during the qualification process in order to accurately evaluate the fracture toughness of the critical grain coarsened area of the HAZ. API RP2Z was suggested as a guideline document for preparation of the weld coupons.

4. Flux cored welding consumables should be procured with fracture toughness data and in one heat or lot if possible to avoid production variation.

5. The lack of skilled PGMAW welders may have a negative impact on schedule.

6. Serious consideration should be given to the usage of the submerged arc process for the skin to flange welds. The submerged arc process would offer advantages of weld quality and productivity for this weld that has less than ideal access for the PGMAW process.

At the request of NASA Glenn NESC engineering staff and Ares I-X Chief Engineer Ada Narvaez-Legeza, ATS Sr. Welding Engineer Michael Hayes visited the Glenn Research Center in Cleveland a second time in May 2007 to meet with key fabrication team members as well as outside consultants to review fabrication procedures for the Ares USS modules. The visit included a tour of the fabrication facility and opportunities to speak with welding technicians and engineers. The following were my primary observations regarding the USS fabrication:

1. The pulsed gas metal arc welding (PGMAW) process was being used for the skin long seam welds and had been qualified. The use of this process for the skin to skin welds was working well and attending the need to weld out-of-position on the Davi rolls. There had been a few weld defects detected by magnetic particle and radiography. These welds may require repair welding and a qualified repair welding procedure must be developed soon. Repairs may need to be done in various positions so the procedure should be qualified in the 6G position to qualify for all possible repair scenarios. The repair welding process should be adaptable to all position welding.
2. There was a continued need to find skilled welders for the pulsed gas metal arc welding process. An outside contractor has been tasked with supplying skilled craftsman. There are few skilled PGMAW welders available for contract work.
3. Welds with straight sided heat affected zones (HAZ) had been produced during the qualification process in order to accurately evaluate the fracture toughness of the critical grain coarsened area of the HAZ and for the weld metal. Mechanical test results from these welds were not yet available as mechanical testing had not been completed. These data are essential for evaluating the fracture toughness of the weld and HAZ and calculation of the critical initial flaw size. Inspection requirements could not be finalized until these results are analyzed.
4. Flux cored welding consumables should be procured with fracture toughness data and in one heat or lot if possible to avoid production variation. The same rationale should apply to all welding consumables purchased for this project.
5. Serious consideration should be given to the usage of the submerged arc process for the skin to flange welds. The submerged arc process would offer advantages of weld quality and productivity for this weld.
6. Experimental work conducted to date on Pathfinder II has illustrated a potential issue with weld fit-up due to irregular plate cutting. This results in varying joint gap and the mechanized pulsed gas metal arc process is not well suited to accommodate even minor changes in joint fit-up.
7. Assuming that procedural changes for more accurate plate cutting and fit-up cannot totally eliminate the joint fit up problems then the project team may want to consider an off-the-shelf joint tracking system to assist the PGMAW

operator. One typical system is the Computer Weld Technology Thru-Arc Tracking system.

8. Weld sequence has been identified as critical for quality and distortion control. There may be significant benefit to welding the fillet weld on the back side of the flange to skin weld before the full penetration mechanized PGMAW weld is deposited. This should facilitate the PGMAW root welding which has been identified by recent inspection to be a potential source of defects such as lack-of-fusion and incomplete penetration.
9. Locating and training skilled welding personnel still seemed to be a problem. This is a problem shared throughout the welding industry. It will most likely be very difficult to find skilled Pulsed Gas Metal Arc welders with mechanized experience.
10. There is a need for a dedicated welding engineer in the Manufacturing Team with direct responsibility and project ownership.

Recent Observations

Shortly after the completion of the fracture toughness testing of the welds produced with the pulsed gas metal arc welding process the manufacturing department decided that it would not be possible to obtain or train skilled operators for the mechanized PGMAW process and switched to the manual semi-automatic flux cored welding process for the flange to skin welds and the skin to skin welds. The initial flux cored welding procedure involved a single sided half V bevel with the bulk of the welding taking place from the outside of the can. Subsequently the project decided to change the weld bevel to ½ half K bevel configuration with balanced welding from the inside and outside of the can to reduce weld induced distortion. The half K configuration has not been tested in fracture mechanics tests to determine what effect if any the change in welding sequence and weld residual stresses may have on the results. Welds made with the current fabrication welding procedure should be tested to confirm that adequate fracture toughness exists to meet the project minimum requirements. We do not know if the double bevel flux cored weld will exhibit the same, worse or better fracture toughness as compared to the single bevel weld primarily as a result of the difference in base metal dilution into the weld metal. The double bevel weld can be expected to have larger portions of base metal chemistry incorporated in the weld metal thus causing a difference in weld metal chemistry and resulting microstructure. Whether or not this change will result in higher or lower fracture toughness can only be determined by testing. The FCAW process is being used in the semi-automatic welding mode and thus there will be variation in welding travel speed and consequently heat input. Welding parameters including travel speed as measured by elapsed time and distance along with arc voltage and welding amperage should be accurately measured for all passes during the test plate welding in order to establish heat input ranges. If the measurements made during the preparation of the test plate reveal a large variation in heat input then testing should be conducted at the high heat input and the low heat input values on separate test plates carefully welded to maintain either the high or low heat input value in order to establish accurate boundary conditions for fracture mechanics testing. On any test plate to be submitted for fracture mechanics testing the following data should be supplied:

- Welding volts per pass
- Welding amps per pass
- Welding travel speed in inches per minute and weld bead width per pass
- Preheat temperature
- Interpass temperature per pass
- FCAW wire identification including AWS class, diameter, and heat or lot number
- Shielding gas flow rates and composition
- Material certifications from the actual heats of base metal and welding filler metals used for the test plate

Wire Type AWS Designation	Mfr and Trade Name	Wire Diameter	Shielding Gas	Welding Position	Heat Input KJ/inch	Base Material	CTOD's Weldmetal Centerline	Test Temp F
E71-T1 12MJ	Hyundai SF7 MC	0.045"	75/25 Argon/CO2	3G	60	API 2H Gr 50	0.037" 0.044" 0.037"	14 14 14
E71-T1	Trimark TM 770	0.045"	75/25 Argon/CO2	3G	40	API 2Y Gr 50	0.059" 0.012" 0.005"	14 14 14
E81-T1-Ni1	Hobart XL8 Ni1	0.045"	75/25 Argon/CO2	3G	50	API 2H Gr 50	0.025" 0.029" 0.033"	14 14 14
E81-T1-Ni1	Hobart XL8 Ni1	0.045"	75/25 Argon/CO2	3G	62	API 2W Gr 60	0.051" 0.051" 0.061"	14 14 14
E81-T1-Ni1	Hobart XL8 Ni1	0.045"	75/25 Argon/CO2	2G	21	API 2W Gr 60	0.032" 0.031" 0.051"	32 32 32

- Welder name and qualifications
- All essential variables required by applicable code and specification

Table G-1.Typical Fracture Toughness Data from Flux Cored Welds

Manual semi-automatic flux cored welds may produce both surface and sub surface weld defects such as slag inclusions, porosity, lack-of-fusion, cracking, and hydrogen embrittlement. The project must use a volumetric inspection technique, preferably ultrasonic testing to find all of these types of defects. Radiography alone would not be sufficient to detect defects such as cracks or lack of fusion depending upon orientation of the defect relative to the x-ray beam.

Welding Processes: The principal welding processes chosen for the Ares Project are:
Semi-automatic Flux Cored Arc Welding (FCAW) Gussets, Flange-to-Flange welds and
Gas Tungsten Arc Welding (GTAW): Root Pass Flange-to-Flange welds. Each of these welding processes is capable of producing quality welds. The level of quality varies from process to process as well as the application of each of these processes to a given weld joint configuration and position. Welder or welding operator skill level with a given process will also play a key role in final weld quality. Training with the exact process, equipment, weld joint and position configuration (i.e. Mock-ups) is essential to achieving adequate weld quality.

Appendix H. NDE Report

Based upon the CIFS predictions shown herein, it appears that if the AIX USS weld design and boundary conditions remain similar to those assumed here, the CIFS will be similar to that predicted within this report. However, if any of the weld design parameters or environmental factors change, such as weld process, cyclic loads and weld toughness measurements, the AIX USS Project should reevaluate the CIFS predictions.

Reliable detection of cracks in materials has been measured for some materials, geometries, surface conditions, and other relevant conditions. The results of these studies were probability of detection (POD) charts that crack detection as a function of crack size for specific test cases and confidence levels. Most of these studies were conducted in the 1970s in support of the developing Space Shuttle Program and are documented in [Ref.1]. The cost of conducting a single POD study on a single geometry and material can substantial as measured in time and money. Manned spaceflight systems components, Space Shuttle Payloads, and associated hardware are required to have a 90 percent probability and a 95 percent confidence level of the CIFS by NASA-STD-(I)-5007. The detection capabilities for standard NDE methods with properly trained and experience inspectors is presented in that can be reasonably be detected based upon Reference 1 are presented NASA-STD-(I)-5009.

Based upon NASA-STD-(I) 5009, a properly conducted UT inspection is capable of detecting embedded cracks larger than 0.164 inches by 0.034 inches with a 90 percent probability and a 95 percent confidence level in wrought material. The geometry of the crack is elliptical. Cracks of equivalent area but different aspect ratios (length / width) will be detectable at a similar level. The radiography testing (RT) detection capability is estimated to be 0.35 inches by 0.35 inches for a 90 percent probability and a 95 percent confidence. Proper RT inspection requires the X-ray beam to be parallel to a crack surface for detection of the crack. For welds this means multiple shots parallel to the weld sidewalls. Therefore, UT is the generally recommended inspection method.

The inspection of weld material can affect the inspection capability. As an example of a way to handle the lack of data on weld defects detectability and the inherent variability of welds consider the way the Space Shuttle External Tank (ET) Project approaches this engineering problem. The ET Project does not use a correction factor for welds on flaw size for an assumed flaw. However, the fracture analysis assumes the flaw exists in the worst possible location and orientation. Those assumptions, combined with the NDE 90/95 assumed crack starting size, and a life factor of four on all loads are considered to be sufficient to cover any concerns of detectability for weld vs. parent material. For actually detected flaws in ET welds, the measured flaw length (2c) is doubled (2X) and an assumed aspect ratio of $a/2c = 0.5$ (where a is the depth of the crack) is used up to 90 percent through-the-thickness at which point the aspect ratio becomes something other than 0.5. Additionally the flaw growth analysis uses upper bound growth and lower bound toughness thresholds and a fracture analysis is performed to assure a safe life of four times the expected use loads, [Ref. 2]. A similar approach has been used by the NESC team for the AIX USS welds to estimate the CIFS.

The CIFS is large enough that the effect of the weld surface and weld metal should not be a concern for detecting critical cracks. Proper UT should adequately detect cracks smaller than the predicted CIFS.

References

1. Nondestructive Evaluation (NDE) Capabilities Data Book (Third Edition) Published by the Nondestructive Testing Information Analysis Center (NTIAC), Texas Research Institute, Austin TX, Nov. 1997.
2. E-mail notes from the MSFC Fracture Control Board Chairman, Gregg Swanson and the MSFC Damage Tolerance Team Leader, Wayne Gregg on July 31, 2007.